Geocenter Motions from GPS: A Unified Observation Model

David A Lavallée[1*], Tonie van Dam[2**], Geoffrey Blewitt[3***], Peter J Clarke[1****]

[1]School of Civil Engineering and Geosciences, [2]European Center for Geodynamics and Seismology , [3]Nevada Bureau of Mines and Geology, and Nevada Seismological Laboratory

*University of Newcastle upon Tyne, NE1 7RU, UK. E-mail: d.a.lavallee@ncl.ac.uk, Telephone: +44 191 222 8203, Fax: +44 191 222 6502.

**Rue Josy Welter, 19, Walferdange, L-7256, Luxembourg. E-mail: tvd@ecgs.lu, Telephone: +352 (33) 14 87 31, Fax: +352-33148788.

***Mail Stop 178, University of Nevada, Reno, NV 89557, United States of America. E-mail: gblewitt@unr.edu, Telephone: +1 (775) 784 6691 ext 171, Fax: +1 (775) 784 1709.

****University of Newcastle upon Tyne NE1 7RU, UK. E-mail: peter.clarke@ncl.ac.uk, Telephone: +44 (0) 191 222 6351, Fax: +44 (0) 191 222 6502.

An edited version of this paper was published by AGU.

Lavallee, D. A., T. van Dam, G. Blewitt, and P. J. Clarke (2006), Geocenter motions from GPS: A unified observation model, J. Geophys. Res., 111, B05405, doi10.1029/2005JB003784.

Abstract

We test a unified observation model for estimating surface loading induced geocenter motion using GPS. In principle this model is more complete than current methods, since both the translation and deformation of the network are modeled in a frame at the center of mass of the entire Earth system. Real and synthetic data for 6 different GPS analyses over the period 1997.25-2004.24 are used to a) build a comprehensive appraisal of the errors and b) compare this unified approach with the alternatives. The network shift approach is found to perform particularly poorly with GPS. Furthermore, erroneously estimating additional scale changes with this approach can suggest an apparently significant seasonal variation which is due to real loading. An alternative to the network shift approach involves modeling degree-1 and possibly higher-degree deformations of the solid earth in a realization of the center of figure frame. This approach is shown to be more robust for unevenly distributed networks. We find that a unified approach gives the lowest formal error of geocenter motion, smaller differences from the true value when using synthetic data, the best agreement between 5 different GPS analyses, and the closest agreement (sub-millimeter) with the geocenter motion predicted from loading models and estimated using SLR. For 5 different GPS analyses, best estimates of annual geocenter motion have a weighted root mean square agreement of 0.6, 0.6 and 0.8 mm in amplitude and 21º, 22º, 22º in phase, for x, y and z respectively.

Geocenter motions, GPS, terrestrial reference frames, mass redistribution

1223 Ocean/Earth/atmosphere/hydrosphere/cryosphere interactions (0762, 1218, 3319, 4550)

1229 Reference systems

1214 Geopotential theory and determination (0903)

1655 Water cycles (1836)

1. Introduction

The mass contained in the Earth's fluid envelope (oceans + atmosphere + continental water) is constant at human timescales. However, its distribution over the surface of the Earth changes continually. Much of this geographic redistribution of surface mass happens periodically at 24 hour to annual periods, and is related to the rotation of the Earth on its axis (e.g. thermally driven atmospheric tides) as well as motion of the Earth around the Sun (e.g. annual global water cycle). In the absence of external forces the center of mass of the entire solid Earth + load system (CM) is a fixed point in space; relative to this point a change in the location of the center of mass of the surface load must (by conservation of linear momentum) induce a change in the relative location of the center of mass of the solid Earth (CE). This "geocenter motion" causes a detectable translation of a geodetic network attached to the solid Earth, relative to the center of satellite orbits, which is CM [*Chen et al.*, 1999; *Watkins and Eanes*, 1993; *Watkins and Eanes*, 1997]. While geocenter motion is principally a product of mass balance relations, the geodetic network is located on the surface of the solid Earth which also deforms due to redistribution of the load. Thus the same process (redistribution of surface mass) is expressed in the geodetic network in two quite different ways: displacement of the Earth's center related to mass balance, and subsequent deformation of the solid Earth due to the load. For a totally rigid Earth there would be no deformation; in an elastic Earth the deformational movement at a point can reach up to 40% of the magnitude of the geocenter trajectory and must be taken in to account [*Blewitt*, 2003]. A graphical representation of these concepts is given in Figure 1.

Estimates of geocenter motion from space geodesy are important since they fundamentally relate to how we realize the terrestrial reference frame [*Blewitt*, 2003; *Dong et al.*, 2003] . Conventionally the center of the International Terrestrial Reference Frame (ITRF) is defined to be at the center of mass of the entire Earth system i.e. CM [*McCarthy and Petit*, 2004]. Estimates of geocenter motion can also help to constrain models involving global redistribution of mass [*Chen et al.*, 1999; *Cretaux et al.*, 2002; *Dong et al.*, 1997] and sea level [*Blewitt and Clarke*, 2003], since they are directly related to the degree-1 component of the surface mass load. This is particularly relevant because current estimates of the degree-1 surface mass load derived from environmental models disagree. A number of authors estimate the annual and semi-annual components of geocenter motion induced by different models of surface mass redistribution [*Bouillé et al.*, 2000; *Chen et al.*, 1999; *Cretaux et al.*, 2002; *Dong et al.*, 1997; *Moore and Wang*, 2003]. While the geocenter motions from different atmospheric mass models tend to agree for all components, significant differences (up to 50%) are observed in annual and semi-annual geocenter motion from ocean bottom pressure and, more importantly, from continental water mass. The standard deviation about the mean of the modeled annual geocenter from 11 different model combinations [*Bouillé et al.*, 2000; *Chen et al.*, 1999; *Cretaux et al.*, 2002; *Dong et al.*, 1997; *Moore and Wang*, 2003] suggests the precision of the modeled annual geocenter variation is of the order ~1mm in amplitude and ~20º in phase.

The Gravity Recovery and Climate Experiment (GRACE) mission results [*Tapley et al.*, 2004] will provide significant new information on the surface mass variations over the Earth down to periods of one month. However, the GRACE products do not include

degree-1 to which GRACE is insensitive. The determination of degree-1 coefficients of the Earth's surface mass load from observational data and the discrimination of modeled environmental data sets is therefore left to other geodetic techniques such as Satellite Laser Ranging (SLR), Doppler Orbitography and Radiopositioning Integrated by Satellite (DORIS) and the Global Positioning System (GPS).

It should be noted that no geodetic estimates of secular geocenter motion currently exist; tectonic deformation will produce a net translation of CF relative to CM which is generally first removed by estimating tectonic velocities at each site. Only if a plate rotation model is used can such an estimate be made and so far is considered systematic reference frame error rather than physical signal [*Argus et al.*, 1999], much further work is required to solve this important reference frame issue. In this work the estimation is considered for the more common use of the term "geocenter motion", i.e. assuming tectonic deformation has been first removed. This work does not reflect the ability of a network shift or Helmert transformation approach to resolve the aforementioned reference frame issues associated with what might be called secular "geocenter motion" or even its ability to resolve secular differences between reference frames.

There have been a number of different approaches to estimating geocenter motions from geodetic measurements [*Ray*, 1999] including (i) the so called "network shift approach" [*Blewitt et al.*, 1992; *Dong et al.*, 2003; *Heflin and Watkins*, 1999] also called the "geometric approach" [*Cheng*, 1999; *Pavlis*, 1999] which directly models the translation between coordinate frames (ii) the "dynamic approach" [*Chen et al.*, 1999; *Pavlis*, 1999; *Vigue et al.*, 1992] which estimates degree-1 coefficients of the

geopotential and (iii) the "degree-1 deformation" approach [*Blewitt et al.*, 2001; *Dong et al.*, 2003] which equates solid Earth deformation caused by the load to geocenter motion. The dynamic and network shift approach are equivalent (where constraints are minimal) and in this work we only consider the latter. We note that describing the "network shift approach as "geometric" is misleading because this approach principally depends on satellite dynamics to locate the Earth Center of Mass and so is fundamentally a dynamic approach. Here we are consistent with the terminology of *Dong et al.* [2003]. *Lavallée and Blewitt* [2002] show that even the non-satellite technique of Very Long Baseline Interferometry (VLBI) is sensitive to geocenter motions via the degree-1 deformation. However, to quote *Boucher and Sillard* [1999], commenting on the geocenter series submitted to the 1999 International Earth Rotation Service (IERS) analysis campaign to investigate motions of the geocenter, "It appears that, even if Space Geodesy geocenter estimates are sensitive to seasonal variations, the determinations are not yet accurate and reliable enough to adopt an empirical model that would represent a real signal." Disagreement between different geodetic analyses is still considerably larger than that between loading models. Much of this disagreement comes from differences between GPS analyses; estimates from SLR tracking of Lageos 1&2 [*Bouillé et al.*, 2000; *Chen et al.*, 1999; *Cretaux et al.*, 2002; *Moore and Wang*, 2003] are in much better agreement.

The source of the disagreement between GPS analyses has been difficult to track down, *Dong et al.* [2002] and *Wu et al.* [2002] estimate the size of the error in the network shift approach due to an imperfect network, and *Wu et al.* [2002] estimate aliasing errors in the degree-1 deformation approach. A number of authors [*Blewitt*, 2003; *Dong et al.*, 2003; *Wu et al.*, 2002] state that the network shift approach is biased by

deficiencies in GPS orbit modeling but a quantitative consideration of how all errors trades off against each other for different networks and approaches has not been completed. Although *Dong et al.* [2003] suggest the degree-1 deformation approach produces more stable geocenter estimates, *Wu et al.* [2002] suggest the ignored higher degrees produce a significant error. This uncertainty in how best to estimate geocenter motions from GPS makes it difficult to recommend procedures for defining the terrestrial reference frame [*Ray et al.*, 2004] or make robust inferences about degree-1 surface mass loading. *Dong et al*. [2003] even suggest that given the improved precision of modern geodetic techniques geocenter motions should be included in the definition of the ITRF as estimable parameters.

Current methods to model geocenter motion consider either the translational or the deformation expression of change in the center of mass of the surface load; here we test a model that unifies these two aspects. In principle this is a better way to model geocenter motions: it is complete, in that all the displacements associated with geocenter motion are modeled, and it is also conventional, such that displacements are modeled in the CM frame. We complete an appraisal of possible errors in the current geocenter motion estimation strategies applied to GPS and make a comparison of the unified approach with these alternatives.

2. Estimating geocenter motions from space geodesy

For mathematical convenience we define "geocenter motion" in the context of this paper as the 3D vector displacement $\Delta\mathbf{r}_{CF-CM}$ of the center of surface figure (CF) of the solid Earth's surface relative to the center of mass (CM) of the entire Earth system (solid Earth,

oceans and atmosphere). Although the term “geocenter motions” has been used to describe the vector difference between a number of frames [*Blewitt*, 2003; *Dong et al.*, 1997], $\Delta\mathbf{r}_{CF-CM}$ or its opposite in sign ($\Delta\mathbf{r}_{CM-CF}$) are the most commonly estimated geocenter parameters from GPS [*Heflin et al.*, 2002; *Malla et al.*, 1993; *Ray*, 1999; *Vigue et al.*, 1992], SLR [*Bouillé et al.*, 2000; *Chen et al.*, 1999; *Cretaux et al.*, 2002; *Moore and Wang*, 2003], and DORIS [*Bouillé et al.*, 2000; *Cretaux et al.*, 2002], so we treat it as the desired estimable parameter. As discussed the center mass of the solid Earth (CE) is displaced from CM due to the changing location of the center of mass of the load. CF is a useful point that represents the geometrical center of the Earth’s surface. It is displaced from CE due to the deformation of the solid Earth accompanying loading; if the Earth were rigid these points would coincide. Since CF is essentially the global average of the surface deformation it differs in location to CE by only ~2% [*Blewitt*, 2003] however this can be misleading since at specific locations the deformational displacement can be of the order of 40%.

The 3-dimensional displacement (east north and up) of a point on the Earth’s surface due to surface mass loading can be described [*Diziewonski and Anderson*, 1981; *Farrell*, 1972; *Lambeck*, 1980] using spherical harmonic expansion and a spherically symmetric, layered, non-rotational and isotropic Earth model of the form

$$E(\Omega) = \frac{\rho_S}{\rho_E} \sum_{n=1}^{\infty} \sum_{m=0}^{n} \sum_{\Phi}^{\{C,S\}} \frac{3l'_n}{(2n+1)} T_{nm}^{\Phi} \frac{\partial_\lambda Y_{nm}^{\Phi}(\Omega)}{\cos\varphi}$$

$$N(\Omega) = \frac{\rho_S}{\rho_E} \sum_{n=1}^{\infty} \sum_{m=0}^{n} \sum_{\Phi}^{\{C,S\}} \frac{3l'_n}{(2n+1)} T_{nm}^{\Phi} \partial_\varphi Y_{nm}^{\Phi}(\Omega)$$

$$H(\Omega) = \frac{\rho_S}{\rho_E} \sum_{n=1}^{\infty} \sum_{m=0}^{n} \sum_{\Phi}^{\{C,S\}} \frac{3h'_n}{(2n+1)} T_{nm}^{\Phi} Y_{nm}^{\Phi}(\Omega) \tag{1}$$

Where T_{nm}^{Φ} are the spherical harmonic coefficients of the surface load density following the conventions of [*Blewitt and Clarke*, 2003] and expressed as the height of a column of seawater, h'_n and l'_n are the degree-*n* Love numbers which for degree 1 must be specified in our chosen frame [*Blewitt*, 2003], ρ_s is the density of seawater and ρ_E is the mean density of the Earth.

It can be shown [*Trupin et al.*, 1992] that surface integration of (1) gives the following geocenter motion between the CM and CF frames:

$$\Delta\tilde{\mathbf{r}}_{CF-CM} = \left(\frac{\left([h'_1]_{CE} + 2[l'_1]_{CE}\right)}{3} - 1 \right) \frac{\rho_s}{\rho_E} \begin{pmatrix} T_{11}^C \\ T_{11}^S \\ T_{10}^C \end{pmatrix} \tag{2}$$

We choose to use CE-frame Love numbers in (2) since the right hand side term in brackets helps demonstrate the concept of translation and then deformation of the solid Earth. The second (unity) term in the brackets is the translation from CM to CE which is much larger than the first term which describes the average deformation of the solid Earth that displaces CF from CE. The first term has a magnitude of 0.021 using the Love numbers of *Farrell* [1972]; it is important to recall however that the deformation at a point given by (1) can be much larger than this.

2.1 A unified observation model

A unified approach for geocenter motion models displacements in the CM frame at each site using the equations in (1), where Love numbers are in the CM frame. In this way both the translation and deformation of the network are modeled. Strictly speaking, only the degree-1 deformation need be modeled as the higher degrees do not relate to the center of mass of the load. Higher degree deformation will however be present in geodetic observations and could alias estimates of geocenter motion if not included, so it can be beneficial to include some of them. For short we call this unified model the "CM method". The design matrix for this approach is given in Appendix A.

A note of caution must be attached to the CM method when anything but a full weight matrix is used during estimation. Estimating the translational aspects of geocenter motions relies on determining the CM frame via simultaneous solution for GPS satellite orbital dynamics and coordinates of a global site network. This information is present in the off diagonal elements of the stochastic model; information on the determination of individual site coordinates relative to the network as a whole is given along the diagonal. It is the stochastic model that determines the relative influence of translation and deformation on the estimate of geocenter motion. If the covariance matrix of observations is diagonal or block diagonal the translation of the network is effectively given a much larger weight than the deformation and the CM method gives identical results to the network shift method

This is particularly pertinent for GPS results obtained using precise point positioning [*Zumberge et al.*, 1997], in which orbits are fixed (considered perfect in the stochastic model). While point positioning is a very useful approach for regional analysis,

it is generally not suitable for estimating global parameters such as geocenter motion. The results obtained will be identical to those from the network shift approach for a global network and the same as common mode filtering [*Wdowinski et al.*, 1997] on a regional scale. *Davis et al.* [2004] attempt to estimate degree-1 deformation from continental-scale point positioning results in this manner so that the remaining higher degree (>1) deformation can be compared to GRACE measurements. However, *Davis et al.* [2004] have removed only a mean from their GPS results (and not the degree-1 deformation), so this is equivalent to common mode filtering on a continental scale.

2.2 The network shift approach

Estimation of $\Delta\mathbf{r}_{CF-CM}$ from GPS measurements has been most commonly performed by modeling displacements as a translation only [*Heflin et al.*, 2002; *Heflin and Watkins*, 1999]. Generally a least squares approach is used to estimate a Helmert transformation with up to 7 parameters [*Blewitt et al.*, 1992]. We follow [*Dong et al.*, 2003] in calling this the "network shift approach". This approach models only the translational aspect of geocenter motions and it is easy to see how such a procedure could be developed from equation (2) since the globally-averaged deformation is very small. Modeling coordinate displacements as only a translation, however, ignores the quite large deformations that can occur on a site by site basis and the estimate in reality defines a center of network (CN) frame [*Wu et al.*, 2002] giving geocenter motion $\Delta\mathbf{r}_{CN-CM}$ which is only an approximation of $\Delta\mathbf{r}_{CF-CM}$.

When estimating a Helmert transformation it can be necessary to estimate rotation parameters since in fiducial-free GPS analysis network orientation is only loosely

constrained [*Heflin et al.*, 1992]; however, a scale parameter should not be estimated. A scale parameter is sometimes included when estimating Helmert transformations to investigate any systematic differences in the definition of scale between different techniques e.g. VLBI, SLR, GPS or DORIS [*Altamimi et al.*, 2002] . When estimating $\Delta\mathbf{r}_{CF-CM}$ however there is no reason to include a scale parameter since we are using only one technique and the scale definition is the same. An estimated scale parameter could absorb some of the loading deformation due to an imperfect (e.g. continentally-biased) network giving an apparent scale error; this error is unfortunate and can be completely avoided by not estimating scale.

2.3 Degree-1 deformation approach

Blewitt et al. [2001] estimate the degree-1 coefficients of the surface mass load (expressed as the load mass moment) from GPS using *a priori* information about the Earth's elastic properties given by the loading model specified in equation (1) and the degree-1 Love numbers of [*Farrell*, 1972] in the CF frame. By modeling only the deformation, the translational aspect of geocenter motion does not influence the estimate. *Blewitt et al.* [2001] model GPS displacements in a realization of the CF frame with

$$\left[\Delta\mathbf{s}_i\right]_{CF} = \mathbf{G}^{\mathrm{T}} diag\left[\left[l'_1\right]_{CF} \quad \left[l'_1\right]_{CF} \quad \left[h'_1\right]_{CF}\right]\mathbf{G}\frac{\mathbf{m}}{M_{\oplus}} \tag{3}$$

Where $\mathbf{m}$ is the "load moment", $\left[h'_1\right]_{CF}$ and $\left[l'_1\right]_{CF}$ are degree-1 Love numbers in the CF frame and for simplification the height and lateral degree-1 spherical harmonic functions

(1) are identified with the elements of the geocentric to topocentric rotation matrix $\mathbf{G}$ (Appendix A). In the notation of this paper this is identical to equations (1) for the CF frame where we identify

$$\mathbf{m}/M_{\oplus} = \frac{\rho_s}{\rho_E}\begin{pmatrix} T_{11}^C \\ T_{11}^S \\ T_{10}^C \end{pmatrix} \tag{4}$$

and hence (3) is a method to estimate $\Delta\mathbf{r}_{CF-CM}$ through equation (2). [*Dong et al.*, 2003] named this the "degree-1 deformation" approach; this is an alternative method to the network shift but is dependent on the specific elastic Earth model (Love numbers) used in (3).

Blewitt et al. [2001] did not provide details on how they realized the CF frame which led [*Wu et al.*, 2002] to incorrectly assume that the results of [*Blewitt et al.*, 2001] were biased by using Love numbers in the CF frame rather than the CN frame. In fact *Blewitt et al.* [2001] used a stochastic approach [*Davies and Blewitt*, 2000] for implicit estimation of translation parameters, which can be shown [*Blewitt*, 1997] to be equivalent to explicit estimation using the functional model;

$$[\Delta\mathbf{s}_i]_{OBS} = \mathbf{t} + \mathbf{G}^{\mathrm{T}} diag\begin{bmatrix}[l'_1]_{CF} & [l'_1]_{CF} & [h'_1]_{CF}\end{bmatrix}\mathbf{G}\frac{\rho_s}{\rho_E}\begin{pmatrix} T_{11}^C \\ T_{11}^S \\ T_{10}^C \end{pmatrix} \tag{5}$$

In this approach the frame-dependent choice of degree-1 Love numbers used in (3) is inconsequential, because the translation parameter $\mathbf{t}$ ensures no-net translation of the network, thus the CN frame is realized. The design matrix for this deformation approach is given in Appendix A.

This approach has the advantages that it is not subject to errors due to approximating $\Delta\mathbf{r}_{CF-CM}$ with $\Delta\mathbf{r}_{CN-CM}$ as in the network shift, and errors in the GPS determination of CM (orbit errors) which map equally (i.e. as a translation) into all site displacements are removed by the translation in (5). Removing common-mode errors in site displacements by estimating a Helmert transformation and expressing displacements in a CN frame is common in GPS analysis [*Davies and Blewitt*, 2000; *Heflin et al.*, 2002; *Wdowinski et al.*, 1997]; however, the residual displacements had not been previously used to estimate degree-1 coefficients of the load. The results are still subject to errors due to the ignored higher degrees in equations (1) [*Wu et al.*, 2002], and GPS observational errors not common to all sites; both errors are of course network dependent.

Dong et al. [2003], *Wu et al.* [2003] and *Gross et al.* [2004] extended this approach to estimate coefficients of the load up to degree 6 using equivalent forms of equation (1). Such an approach should reduce the errors in the estimate of degree 1 which may exist in the estimates of *Blewitt et al.* [2001] caused by ignoring the higher degrees [*Wu et al.*, 2002]. Additionally estimating higher degree terms, however, requires a dense and well distributed network.

In their estimation procedure both *Dong et al.* [2003] and *Wu et al.* [2003] place their observations in the CN frame by first removing a 7 parameter Helmert transformation and estimating loading coefficients from the residuals. Both these results

could be biased downwards due to the inclusion (and subsequent removal from the displacements) of a scale parameter.

3. GPS error analysis

In order to fully test the different techniques for estimating geocenter motion we first investigate the likely error sources involved. Errors are highly network dependent so it is crucial to considering different (but realistic) networks. The likely errors naturally fall into two categories: random and systematic GPS technique-specific errors, and systematic errors due to mismodeling of the loading deformation. Random errors are considered in section 3.3 by propagation of the GPS formal error. The systematic effects of mismodeling are considered in section 4 by creating synthetic GPS data sets with known statistical properties so that the estimated value can be compared to the "true" value used to create the data. The effects of GPS-specific systematic errors are difficult to analyze here, orbit errors tend to affect the z component more than x or y since they are modulated by Earth rotation [*Watkins and Eanes*, 1994] and some degree of uncertainty in geocenter motion is attributable to not resolving ambiguities. Other GPS-specific systematic errors are also likely, such as second-order ionospheric effects [*Kedar et al.*, 2003] and tidal aliasing [*Penna and Stewart*, 2003]; however their consideration is beyond the scope of this paper and we concentrate on the systematic errors, which are generated by the loading deformation itself, due to mismodeling.

3.1 GPS data

We use global GPS data from six International GNSS Service (IGS) analysis centers over the seven-year period 1997.25-2004.25: GeoForschungsZentrum (GFZ), the European Space Agency (ESA), the NASA Jet Propulsion Laboratory (JPL), Natural Resources Canada (EMR), the US National Geodetic Survey (NGS) and Scripps Institution of Oceanography (SIO). Weekly coordinate Solution INdependent EXchange (SINEX) files [*Blewitt et al.*, 1994] from each analysis center are produced and archived each week as part of routine IGS activity. Each SINEX file contains a precise and rigorous estimate of the IGS polyhedron, using the most up to date methods and techniques [*Blewitt et al.*, 1994]; the orbit, timing and coordinate products from both the IGS and individual analysis centers are used in much of the ongoing global and regional scientific GPS processing, and the analysis center solutions are a core contribution to the ITRF.

Each IGS analysis center processes its own particular subset of the IGS network, using software which can have quite different approaches to determining site coordinates from GPS data. As such they provide an ideal data set for exploring the errors in geocenter motions and the best method to estimate them, since the major processing software and strategies are represented yet produce solutions from the same GPS data. Most importantly the SINEX format allows for complete archival of estimated site coordinates, the full variance-covariance matrix and the full set of applied constraints; these constraints can be subsequently removed to produce “loose” or “free” networks [*Davies and Blewitt*, 2000; *Heflin et al.*, 1992]. This is important since we wish to assess the determination of geocenter motions free from any particular frame that the individual analysis center has chosen to represent its weekly coordinates. Once these constraints are removed, the SINEX files form GPS realizations of the CM frame.

Velocities are estimated and removed from the analysis center solutions using a consistent rigorous least squares strategy with full covariance information [*Davies and Blewitt*, 2000; *Lavallée*, 2000]. Sites with less than 104 weekly observations over 2.5 years are rejected. Two and a half years is chosen to eliminate velocity errors associated with annual signals [*Blewitt and Lavallée*, 2002]. Outliers and data segments with known problems are rejected, and offsets due to equipment changes (particularly radome and antenna changes), earthquakes or site moves are estimated. The analysis centers ESA and SIO do not apply the pole tide correction so this is applied using IERS standards [*McCarthy and Petit*, 2004].

To maintain a consistent level of formal error scaling, the input weight matrices are scaled by the unit variance (chi squared per degree of freedom) in the case where residuals are estimated assuming the network shift approach, which is standard in GPS analysis. It is difficult to ascertain whether formal errors will be overestimated or underestimated in this case. If un-modeled observational errors are larger than the real geophysical loading then errors will be underestimated; conversely if the loading dominates then this approach could overestimate the errors. We take this scaling to be at least a commonly-accepted approach.

3.2 Networks

The estimation of geocenter motions is fundamentally linked to the representation of the Earth's surface using a geodetic network. Network size and distribution are therefore key factors in the error assessment of different methods. The analysis centers have different approaches to choosing the weekly subset of the IGS global network they analyze. Figure

2 shows the number of sites analyzed each week after the rejections necessary to estimate velocities mentioned above. Some analysis centers such as EMR restrict their analysis to a small number of sites whereas SIO maintain an analysis that more closely mirrors the overall growth of the IGS network. A crude but informative way to assess network distribution, particularly in the context of geocenter motions, is to look at the percentage of sites within opposing hemispheres centered on the direction of each Cartesian axis. Figure 3 plots the percentage of sites in the hemisphere centered upon each coordinate axis, the center line at 50% represents an "ideal" equally distributed network. Although there are a number of factors, the distribution of a realistic global geodetic network is governed primarily by the ocean-land distribution (~ 70% of the Earth's surface is ocean). Figure 3 clearly reflects this: the inequality between the North and South hemispheres in the z direction is the largest, reaching up to almost 80% of sites in the Northern hemisphere, 30% larger than the "ideal". The inequality in the x and y directions varies up to only 15% yet there is still a noticeable tendency towards sites being located in the hemisphere centered on the x axis (Europe) and the hemisphere centered on the negative y axis (N America). JPL maintain the best north-south distributed network in this simple analysis but only at the expense of network size. What is clear is that although the IGS network is growing considerably the distribution is not improving at the same rate, and realistically this is always likely to be the case due to the ocean-land distribution. There is always a trade-off between reducing random error by increasing network size, and possibly introducing systematic error in the geocenter motion estimates by degrading distribution. The best method for determining geocenter

motions from space geodesy should therefore be able to take advantage of improved network size without necessarily better distribution.

3.3 Propagation of observational formal errors

Assessment of how the GPS formal errors map into each estimate is performed by propagating the formal covariance matrix of the observations to the covariance matrix of the parameters in each method. The scaling of the formal covariance matrix from each of the different analysis centers relates to the *a priori* variance assigned to the initial GPS phase estimate and any other scaling applied during the GPS processing, so it would be unwise to interpret the scaling of formal errors between analysis centers in detail. It is also unnecessary; it is the relative scaling, i.e. the performance of each geocenter estimation method, that is of concern.

Figures 4 and 5 plot the changes in formal errors over time, for two end-member cases of network size/distribution during the interval 1997.25-2004.25. The higher degrees are ignored in the degree-1 deformation and combined approaches for the time being, Table 1 lists the mean formal error over the interval for each component (x, y and z), method, and analysis center. The strength of an approach in dealing with different networks is reflected in the similarity between the $\mathbf{r}_{CF-CM}$ x, y and z formal error; in a robust approach the formal error on the geocenter will be the same in all directions whatever the network distribution.

Figure 4 shows the formal error in the JPL geocenter x, y and z components from each of the three methods for this interval. The formal error in all approaches reduces with time; this to some degree reflects improvements in GPS software models, but mostly

reflects the increase in size of the GPS tracking network (Figure 2) which is about 100% over the entire interval. The distribution of the network (Figure 3) remains relatively well balanced and consistent over time and this is reflected in the formal errors for the network shift approach being roughly identical in x, y and z directions (Figure 4 and Table 1). The network shift method is predicted to perform slightly better than the degree-1 deformation approach for all components. In part this is due to dilution of precision: it is necessary to estimate 3 extra translation parameters in the degree-1 deformation approach. Of most interest is that the CM approach is predicted to give mean formal errors between 42-52% smaller than either the network shift or degree-1 deformation approaches.

Figure 5 shows the formal error in the SIO geocenter x, y and z components from each of the three methods for the same interval. The results are quite different to those of the JPL network since the SIO network includes more sites (Figures 2 and 3). In this case the most noticeable effect is the poor performance of the network shift. Because of the uneven network, the z component of geocenter formal error is approximately 3 times that in the x and y (Figure 5). The degree-1 deformation approach however performs much better with both smaller and virtually identical formal errors in all directions (Figure 5 and Table 1). The CM approach again improves the formal errors in all directions. The improvement in mean formal error in x, y and z respectively is 2%, 72%, and 69% over the degree-1 deformation approach, and 16%, 44%, and 83% over the network shift approach.

Figures 4-5 and Table 1 demonstrate that the network shift approach should perform well when a network is well distributed, in fact as well as the degree-1

deformation approach (although this does not include the error in assuming $\mathbf{r}_{CF-CM} = \mathbf{r}_{CN-CM}$ or aliasing effects) but when a network is poorly distributed the degree-1 deformation approach should be far superior. This can explain the observation that the degree-1 deformation approach produces geocenter motions that are more stable with time [*Blewitt et al.*, 2001; *Dong et al.*, 2003], since the degree-1 deformation approach should perform much better as network distribution changes. The CM approach is predicted to perform considerably better than either approach (Table 1) despite the network distribution; in principle this will always be the case as the information content of both the other approaches is used. This suggests that it may be possible to exploit the improvement in IGS network size with time despite the relatively small improvement in N-S distribution.

4. Analysis of geocenter motion mismodeling errors

4.1 Synthetic data

Synthetic GPS data are created by adding displacements predicted by a hydrological loading model to site positions specified by the analysis center networks. We use surface atmospheric pressure from the National Center for Environmental Prediction (NCEP) reanalysis data set [*Kalnay et al.*, 1996]. The data are provided on a 2.5 degree x 2.5 degree global grid at 6 hourly intervals. We average 7 days of data (28 epochs) centered on the GPS week corresponding to the SINEX files. The ocean is treated as a pure inverted barometer; that is, we set the pressure to zero over the oceans.

For the ocean bottom pressure, we use values derived from a simulation of the oceans completed at JPL as part of their involvement in the Estimating the Circulation

and Climate of the Ocean (ECCO) consortium [*Stammer et al.*, 1999]. The ocean model used in this simulation spans the globe between 77.5º south and 79.5º north latitude with a latitudinal grid-spacing ranging from 1/3º at the equator to 1º at high latitudes and a longitudinal grid-spacing of 1º. The model is forced twice daily with wind stress and daily surface heat flux and evaporation-precipitation fields from the NCEP/NCAR reanalysis project. The 12-hourly data was averaged into weekly values.

We use continental water storage variations derived from simulations of global continental water and energy balances, created by forcing the Land Dynamics (LaD) model [*Shmakin et al.*, 2002] with estimated atmospheric variables. The water storage data (snow, groundwater and soil moisture) are provided at 1° x 1º global resolution at monthly time periods. The most recent version of the model, LaD World-Danube, extends from January 1980 to April 2004. The monthly data were linearly interpolated to weekly values.

The total load is made gravitationally self-consistent and mass-conserving by adding a spatially-variable surface mass layer over the oceans [*Clarke et al.*, 2005]. This amplifies the annual degree-1 component of the load and also $\Delta\mathbf{r}_{CF-CM}$ by 26%, 13% and 17% in x, y and z components respectively (Table 2). Figure 6 and Table 2 summarize the total load. The power spectra of the model-predicted geocenter motion are plotted in Figure 6. The overwhelming majority of spectral power is at the annual frequency since geocenter motion is driven by the seasonal water cycle. A small amount of power exists at the semi-annual frequency in the z component. The variance reduction when fitting a pure annual signal to the x, y and z total load is 65%, 70% and 53% respectively. This is the reason that most work [*Bouillé et al.*, 2000; *Chen et al.*, 1999; *Dong et al.*, 1997;

Dong et al., 2003; *Moore and Wang*, 2003] concentrates on the annual component of geocenter motion and if only to avoid plotting a very large number of time series we also consider the annual signal for inter-comparison purposes.

A synthetic loading deformation dataset is produced for each analysis center by creating correlated Gaussian normal deviates with a mean centered on the predicted deformation and variance- covariances obtained from the full weekly SINEX formal covariance matrices. We assume that the SINEX covariance matrices represent a reasonable assessment of the random errors and a much better approximation than uncorrelated errors with a blanket value for the noise in each east, north and up component. The synthetic dataset now includes specified random errors and can be used to investigate how the random errors expected in $\Delta\mathbf{r}_{CF-CM}$ (section 3.3) combine with systematic effects from mismodeling and site network distribution.

4.2 Errors due to approximation of $\mathbf{r}_{CF-CM}$ with $\mathbf{r}_{CN-CM}$

The network shift approach will always be sensitive to systematic error so long as the satellite tracking network incompletely samples the Earth's surface. The size of this error depends on the network distribution and observational errors, *Wu et al.* [2002] estimate this error for the 30-site SLR network of [*Bouillé et al.*, 2000] to be approximately 1 mm, *Dong et al.* [2002] also find this error to be sub-millimeter. In both cases uncorrelated errors are assumed. Whilst 1 mm is still significant when the modeled signal is of the order 3-4 mm [*Chen et al.*, 1999; *Dong et al.*, 1997; *Moore and Wang*, 2003], assuming uncorrelated errors is likely to seriously underestimate the error when estimating the mean site displacement if real correlations exist . We compute this error for each analysis

center network series using correlated synthetic data. The results are plotted in Figures 7 and 8 and discussed in section 4.4 below.

4.3 Errors due to higher degrees of loading

The degree-1 deformation and CM approaches are not subject to errors in approximating $\mathbf{r}_{CF-CM}$ with $\mathbf{r}_{CN-CM}$ since the deformation is modeled at each site (i.e. in the CN frame); however only the degree-1 deformation is modeled, and degrees > 1 are ignored. Ignoring these higher degrees could cause significant aliasing into the estimated geocenter motion [*Wu et al.*, 2002]. *Wu et al.* [2002] conduct a sensitivity analysis to estimate geocenter motion annual amplitude, and consider uncertainties for the 66-site network of *Blewitt et al.* [2001] to be (9, 8, 10) and (3, 2, 9) mm in x, y and z respectively for two different load scenarios. *Wu et al.* [2002] scaled the degree 2-50 coefficients in their load scenarios by 6.6, the load moment z component of *Blewitt et al.* [2001]. *Wu et al.* [2002] may have overestimated the effects of aliasing with such a scaling, especially since the load moment results of *Blewitt et al.* [2001] were likely already aliased.

We compute the aliasing error for each analysis center network series, the degree-1 deformation and CM approaches using the correlated synthetic data. The results are plotted in Figures 7 and 8 and discussed in section 4.4 below.

4.4 Results

Estimates of the two mismodeling errors discussed in sections 4.2 and 4.3 are plotted alongside each other in Figures 7 and 8; values estimated from the synthetic data sets are compared with the “true” values used to create the data. This way the systematic errors

introduced in the network shift approach by approximation of CF with CN can be contrasted with the systematic errors introduced in the degree-1 deformation and CM approaches by higher degree aliasing. Observational random errors (section 3.3) are the same for all methods as they are specified by the synthetic data.

Previous work with uncorrelated synthetic data [*Dong et al.,* 2002; *Wu et al.*, 2002] suggests that annual mismodeling errors are on the order of ~1 mm for the network shift approach and up to ~6 mm in the degree-1 deformation approach; similar results have been obtained with uncorrelated data by the authors of this paper. Such results can however be misleading, since global GPS solutions will have correlated random errors. If we look at our synthetic data set where inter-site correlations are considered (Figures 7 and 8) a very different picture emerges, in this case network shift annual amplitude can vary from the true value by as much as ~4 mm in x and y, up to 10 mm in z, and between analysis centers by almost as much. The phase variations are even more extreme with some phases shifted almost 180º from both the true value and between analysis centers. These results indicate that correlated errors in global geodetic solutions could cause significant errors and disagreement between estimates of geocenter motion when using the network shift approach (particularly when using different networks); this error is much larger than aliasing effects in the deformation approach. This conclusion is enhanced by the poor agreement between GPS geocenter motion estimates using the network shift approach [*Ray*, 1999] and observations that the degree-1 deformation approach produces more stable results [*Dong et al.,* 2003].

The degree-1 deformation method produces better results than the network shift approach (Figures 7 and 8), with annual amplitudes that are generally closer to the true

value and in better agreement between different networks (particularly in z). The improvement in phase stability is quite considerable. Aliasing of higher degrees still has an effect and the best degree-1 deformation results are achieved when degree-2 is also estimated; in this case errors are up to 0.8, 0.9 and 2.6 mm in x, y and z amplitudes respectively, in phase, errors are up to 31º, 42º and 26º respectively.

The CM method consistently produces results which are closer to the true value than either the network shift or degree-1 deformation approaches (Figures 7 and 8). When degree-2 is also estimated, amplitude errors are predicted to be up to 0.5, 0.3 and 2.5 mm in x, y and z respectively; if the network is well distributed then the error in z can be as low as 0.6 mm. Phase errors are predicted to be up to 22º, 26º and 28º in x, y and z respectively. The method is in principle the best way to model the observations and from this simulated analysis is indeed the best performer.

It can be observed that for all methods the SIO network produces results in amplitude and phase that are usually furthest from the true value, particularly when degree-2 is not estimated. This network contains a large number of regional sites and demonstrates the effects of a very uneven network. It is unlikely that such sites would normally be included in a geocenter estimation analysis; however, inclusion of these sites provides a useful end member estimate of the errors. For such a large network it is possible to estimate spherical harmonic degrees greater than 2 with the deformation approaches [*Wu et al.*, 2003]. Only the SIO network is really large enough to do this reliably (Figure 2). We estimate up to degree 6 with the degree-1 deformation approach and CM approach from the synthetic data, in this case we find that the annual x and y amplitudes do not get any closer to their true values compared to the case when only

degrees 1 and 2 were estimated, but the SIO z amplitudes now varies from the true value by only 0.4 mm, an improvement of 84%, with the annual phase hardly effected. This suggests that, whilst aliasing from degrees beyond 2 is minimal for x and y, the tendency for an uneven network in the z direction requires higher degrees to be estimated to overcome aliasing, and that this may be a viable approach for large but regionally dense networks such as SIO.

5 Network scale

It is common when estimating Helmert transformations to estimate a scale parameter [*Heflin et al.*, 2002]. In the case of an uneven network this scale parameter could absorb some of the real deformation due to surface mass loading, and is unnecessary when geocenter motions are estimated. This effect has been found significant for the network shift approach with noise-free, uncorrelated synthetic site data from just atmospheric pressure loading [*Tregoning and van Dam*, 2005]. The effect on the estimated $\Delta\mathbf{r}_{CF-CM}$ of including a scale parameter is investigated here, for correlated and noisy synthetic data from the entire surface load and additionally real GPS data.

With the synthetic data, estimating scale has the largest effect on $\Delta\mathbf{r}_{CF-CM}$ estimated using the network shift approach. This effect is very significant in the z component; the annual amplitude is altered by up to 0.33, 0.16 and 1.5 mm in x, y and z components respectively. When using either of the deformation approaches the z component changes only up to 0.4 mm, phase differences are at most 3º for x and y with a network shift z value of 10º .

For the real data the picture is very similar: the effect on the estimated $\Delta\mathbf{r}_{CF-CM}$ is significant with a maximum effect on annual amplitude of 1.29 mm in x, 2.11 mm in y and 4.6 mm in z. These differences are again maximal for the network shift approach; for the unified approach, the maximum effect is 0.86, 0.81 and 3.23 mm in z. The effect on annual phase can reach 68º in x with the network shift method.

The size of the estimated scale parameter is also significant. In the synthetic data there is no true scale variation, only scale error arising through the interaction between loading and network geometry. Figure 9 plots the power spectra of the scale series estimated for each method (network shift, degree-1 deformation etc.), averaged over all analysis centers. The averaging is simply for clarity, the same observations are made from each individual analysis center scale spectrum. In the synthetic data (Figure 9a), the scale series power spectrum is flat with a sharp peak at the annual frequency; this is largest (and significant at 5%) for the network shift approach and gets progressively smaller (and no longer significant) when using the degree-1 deformation and CM approaches respectively. If degree-2 is included in these latter methods then it gets smaller still. Figure 9b also plots the power spectra of the scale estimated from the real data, there is a clear annual peak which is largest for the network shift approach and reduces in amplitude when increasing amounts of the loading deformation are estimated. The mean amplitude of seasonal scale estimated from the network shift approach is 0.15 ppb for the synthetic data and 0.37 ppb for the real data. It is likely that the observed seasonal changes in scale of 0.37 ppb and other results of the order 0.3 ppb [*Heflin et al.*, 2002] are due to aliasing of the loading signal. It is encouraging to realize that the

seasonal signals observed in GPS scale are at least partly due to a real loading signal rather than any particular GPS specific systematic error.

Another possible scale error exists when results are put in the CN frame using a 7 parameter Helmert transformation and then the residuals are used to estimate the deformation due to surface loading with the degree-1 deformation approach [*Dong et al.*, 2003; *Wu et al.*, 2003]. In this scenario it is possible that the estimation and subsequent removal from the data of a scale parameter could also remove some actual deformation due to loading. We estimate the size of the error in geocenter motions estimated this way from the synthetic data to be up to 1.84 mm in annual amplitude and up to 40º in phase. With the real data, using such a two-step procedure can change the estimates by as much as 4.3 mm in annual amplitude and 85º in phase. The effect of this two-step approach is generally to reduce load amplitude since some of the power is absorbed by the scale parameter; It is likely that this accounts for the significant reduction in annual degree-1 amplitude observed by *Dong et al*. [2003] compared to *Blewitt et al*. [2001].

6. Comparison of estimated geocenter motion

Geocenter motions for the period 1997.25-2004.25 are estimated from the GPS solutions for each of the 6 IGS analysis centers. Annual amplitude and phase are shown in Figures 10 and 11; for comparison the predicted values from the loading model are also given. Comparing these solutions gives insight into both network and modeling effects; each analysis center has used the same GPS data but sometimes very different networks, analysis software, and procedures. The most noticeable result of this analysis is the large disagreement between analysis centers in geocenter motion annual phase for the network

shift approach z component (Figure 11), this can be as large as 166º and apart from one comparison is always greater than 50º. Such a situation is predicted by the simulated data (section 4.4, Figure 8) and results from a very uneven network in the z direction. This result combined with that from the synthetic analysis clearly explains the disagreement previously seen amongst GPS estimated geocenter motions using the network shift approach [*Ray*, 1999]. Furthermore it suggests serious shortcomings in the network shift approach for estimating geocenter motions from GPS. In addition to network effects, one possible explanation is the different strategies taken to ambiguity fixing however only JPL resolve all ambiguities; the other analysis centers fix some or none at all and no consistent differences are observed in Figures 10 & 11.

The two deformation methods give considerably better agreement in phase (Figure 11); in fact, the estimates of annual phase from these methods appear to be much less affected by aliasing, network size, and distribution than is the estimated annual amplitude, another result predicted by the simulated data analysis. The Weighted Root Mean Square (WRMS) annual phase values (about the weighted mean) are around 15º in all components for the CM and degree-1 deformation methods compared with 15º, 17º and 108º in x, y and z for the network shift method (Table 3).

In Figure 10 the solution for ESA is in disagreement with the other analysis centers for all approaches; the reason for this is unknown. If we treat this solution as an outlier and exclude it, then annual amplitude agreement between the remaining 5 analysis center solutions is much improved (Table 3).

The deformation methods are affected by aliasing. If degree-2 is also estimated then the deformation methods perform much better in amplitude as predicted by the

simulated results, particularly for the large network SIO (Figure 10). The SIO network is very unevenly distributed, not normally a choice for estimating geocenter motions or defining a frame. If we restrict ourselves to “reasonable” networks only (the remaining 4 analyses) then the network shift method gives WRMS amplitude variation of around 1.5 mm, the degree-1+2 method has a larger z agreement, but by far the best performance is achieved when using the CM + 2 approach: WRMS variation is entirely sub-millimeter at 0.6, 0.6 and 0.3 mm in x, y and z (Table 3). In this context “reasonable” means that clustering in one axis centered hemisphere is limited to less than 70% of sites (Figure 3).

The simulated analysis (section 4.4) and *Wu et al*. [2003] suggest that estimating additional higher degrees of the load may overcome the problems of an uneven network. We estimate degrees 1 through 6 for the SIO network. In this case the WRMS variation in x, y and z amplitude is 0.6, 0.6 and 0.8 mm for the CM approach (Table 3). These results suggest that estimating higher degrees in the CM frame is a valid approach to take for large unevenly distributed networks; it performs almost as well as when using evenly distributed networks and just estimating degrees 1 and 2. Table 3 also suggests that modeling higher degree deformations in the CM rather than CN frame gives improved results. Removing higher degree deformations using GRACE results, [*Davis et al.,* 2004], is another approach that may improve geocenter estimates; however, this would not be possible prior to 2002. In section 2.1 it was stated that the CM method reduces to the network shift method in the case of a diagonal or block diagonal weight matrix. This is easily verified and has been done for the results presented here; the CM and network shift methods produce near identical results in this case.

The estimated annual amplitude and phase are compared with those predicted by the load model (section 4.1). Horizontal dashed lines representing the load model values are included in Figures 10 and 11, and the mean estimated values in Table 3 can be compared with the loading model predicted values in Table 2. In this comparison the CM method where degree-2 is also estimated is in best agreement with the loading model; consistently the annual amplitude and phase are closer to that predicted by the loading model than any other method, whether SIO is included or not (still treating ESA as an outlier). Excluding SIO and ESA, agreement of the weighted mean annual amplitude with the load model is 0.09, 0.95 and 0.91 mm. If degrees up to 6 are estimated from SIO then the results are only slightly different (Table 3). Phase differences with the load model are 14º, 3º and 35º in x, y and z respectively. These difference are much larger than our formal errors (Table 3); however, if only because of aliasing, the formal errors are obviously too small. An improved estimate of the observational errors comes from the WRMS agreement between the analysis center values (Table 3). In this case the load model falls within 2 standard deviations of the CM approach best-estimate (mean of 4 analysis centers).

The annual amplitude and phase are also compared to network shift results from SLR tracking of Lageos 1&2 [*Bouillé et al.*, 2000; *Chen et al.*, 1999; *Cretaux et al.*, 2002; *Moore and Wang*, 2003]. The 4 SLR results are in very good agreement with a mean annual amplitude 2.60, 3.00 and 3.55 mm, mean phase of 221º, 130 º and 219 º, RMS amplitude of 0.56, 0.86 and 0.66 mm and RMS phase of 13º, 11º and 5º in x, y and z respectively. Compared to the best estimates from GPS using the CM+2 approach (Table 3) SLR has near identical annual amplitude RMS but half that achieved by GPS in annual

phase RMS. It is clear that the SLR results do not have the same errors in the network shift as GPS; the improved sensitivity of Lageos 1&2 to the geocenter means the combination of observational and approximation errors (CF with CN) are smaller. The systematic error from approximating CF with CN still exists however, and since the SLR tracking network does not vary to the degree GPS does, is likely similar between estimates. The CM approach could improve SLR geocenter estimates still further.

The mean SLR result is plotted on Figures 10 & 11, differences between the mean SLR estimate, the best GPS mean estimate (CM+2) and the loading model are insignificant at 2 sigma when the RMS is used as an estimate of formal error. At the 1 sigma level there is a significant discrepancy between the geodetic measurements (which agree) and the load model in z amplitude and the y annual phase from SLR is significantly different from both GPS and the load model.

The considerably improved precision of the CM approach is still not small enough to reliably discriminate between different load models; however, the level of agreement between geodetic estimates of geocenter annual motion (Table 3) is now about the same level as that between different load models, a considerable improvement in observational precision over that previously seen from GPS.

7. Conclusions

Historically the “network shift” approach has been the most commonly used approach to estimating geocenter motions from geodetic data. We find that it has a number of shortcomings when applied to GPS. Estimated and predicted results from synthetic data demonstrate that the geocenter annual phase estimated by the network shift is particularly

unstable. Significant levels of seasonal scale variation observed in GPS analysis are at least in part due to the interaction of surface mass loading with a sparse geodetic network, and mis-modeling of the Earth's degree-1 deformations with the network shift approach. Scale should not be estimated with geocenter motions, or biased results will be obtained.

Alternative approaches for estimating geocenter motions with GPS have involved modeling the degree-1 (and sometimes higher) deformations in realizations of the CF frame [*Blewitt et al.*, 2001; *Dong et al.*, 2003; *Wu et al.*, 2003]. In terms of formal error, modeling the deformations in this way is much more robust when networks are uneven. Aliasing from un-estimated higher degrees, although important, can be alleviated by estimating the total load to degree 2, but in the case of very large unevenly distributed networks even higher degrees must be estimated.

In principle an approach that unifies both the translation and deformation aspects of geocenter motion is more complete, should take advantage of all GPS information content, and is conventional since all deformations are modeled in the CM frame. Such an approach is found to give the lowest geocenter motion formal error, smaller differences from the true value when using synthetic data, the best agreement between 5 different GPS analyses and the closest agreement with the geocenter motion predicted from loading models and estimated from SLR.

A note of caution must be attached, however: unless the unified (CM) method uses a full weight matrix that is obtained from simultaneous estimation of station coordinates with orbit parameters, the relative weight of information between the translation and deformation would be incorrect. For example, using the covariance matrix

from precise point positioning (which fixes the orbits) would be inappropriate, and would produce nearly identical, poorer results to the network shift approach.

With this newest approach, provided care is taken to ensure a balanced network or higher degrees are estimated as required, we demonstrate that it is possible to estimate geocenter motions from GPS with unprecedented sub-millimeter levels of precision. This level of precision is still however insufficient to reliably discriminate between different loading models. Geocenter motion agreement between different GPS solutions is now at the same level as geocenter motion agreement between different loading models. With improved GPS error modeling and mitigation, reprocessing of older data and further placement of GPS sites in the southern hemisphere, a level of precision that can in the near future discriminate between load models does now appear possible.

Appendix A: Least Squares design matrices.

CM approach

Displacements are modeled completely in the CM frame using equations (1) and Love numbers in the CM frame. The parameter vector is

$$\mathbf{x} = \begin{pmatrix} r_x & r_y & r_z & \Delta\mathbf{r}_{CF-CM} & T_{22}^C & T_{22}^S & T_{21}^C & T_{21}^S & T_{20}^C & T_{\bar{n}0}^C \end{pmatrix}^{\mathbf{T}} \tag{A1}$$

Where r are rotation parameters, $\Delta\mathbf{r}_{CF-CM}$ is the geocenter motion, and T_{nm}^{Φ} are spherical harmonic coefficients of the higher degrees (>1) of the total surface load. The choice to include higher degrees is optional. The least squares design matrix for i th site is

$$\mathbf{A}_i = \begin{pmatrix} 0 & z & -y & \left(\frac{3}{([h'_1]_{CE} + 2[l'_1]_{CE})} - 1\right)\mathbf{G}_i^{\mathbf{T}} diag\begin{bmatrix}[l'_1]_{CM} & [l'_1]_{CM} & [h'_1]_{CM}\end{bmatrix}\mathbf{G}_i & \mathbf{B}_i \\ -z & 0 & x & & \\ y & -x & 0 & & \end{pmatrix} \tag{A2}$$

where $\mathbf{G}_i$ is the 3×3 matrix that rotates geocentric into topocentric displacements (east, north and up) about a point with latitude φ and longitude λ.

$$\mathbf{G}_i = \begin{pmatrix} -\sin\lambda & \cos\lambda & 0 \\ -\sin\varphi\cos\lambda & -\sin\varphi\sin\lambda & \cos\varphi \\ \cos\varphi\cos\lambda & \cos\varphi\sin\lambda & \sin\varphi \end{pmatrix} \tag{A3}$$

The matrix $\mathbf{B}_i$ contains the partial derivatives for higher degrees (>1) from equation (1).

Network shift approach

Generally a least squares approach is used to estimate a Helmert transformation with up to 7 parameters

$$\mathbf{x} = \begin{pmatrix} t_x & t_y & t_z & s & r_x & r_y & r_z \end{pmatrix}^{\mathrm{T}} \tag{A4}$$

where the parameter $\hat{\mathbf{t}} = \begin{pmatrix} t_x & t_y & t_z \end{pmatrix}^{\mathrm{T}}$ is the least squares estimate of $\Delta\mathbf{r}_{CF-CM}$ and s is an optional scale parameter, the design matrix is

$$\mathbf{A}_i = \begin{pmatrix} 1 & 0 & 0 & x_i & 0 & z_i & -y_i \\ 0 & 1 & 0 & y_i & -z_i & 0 & x_i \\ 0 & 0 & 1 & z_i & y_i & -x_i & 0 \end{pmatrix} \tag{A5}$$

Degree-1 deformation approach

In the degree-1 deformation approach the parameter vector is

$$\mathbf{x} = \begin{pmatrix} t_x & t_y & t_z & r_x & r_y & r_z & \Delta\mathbf{r}_{CF-CM} & T_{22}^C & T_{22}^S & T_{21}^C & T_{21}^S & T_{20}^C & \cdots & T_{\bar{n}0}^C \end{pmatrix}^{\mathrm{T}} \tag{A6}$$

With translation t and rotation r (which are both discarded), geocenter motion $\Delta\mathbf{r}_{CF-CM}$ and higher degrees up to degree $\bar{n}$ of the surface mass load, the design matrix is

$$\mathbf{A}_i = \left(\begin{array}{ccc:ccc:c:c} 1 & 0 & 0 & 0 & z & -y & \left(\dfrac{3}{([h'_1]_{CE} + 2[l'_1]_{CE})} - 1\right)\mathbf{G}_i^{\mathrm{T}} diag[[l'_1]_{CF} \quad [l'_1]_{CF} \quad [h'_1]_{CF}]\mathbf{G}_i & \mathbf{B}_i \\ 0 & 1 & 0 & -z & 0 & x & & \\ 0 & 0 & 1 & y & -x & 0 & & \end{array}\right)$$

(A7)

Acknowledgements

We thank the IGS analysis centers for providing the SINEX solutions used in this work. We would like to thank Yehuda Bock, Erricos Pavlis and Mike Watkins for constructive reviews. The authors acknowledge a Royal Society University Research Fellowship to DAL and funds from the Luxembourg government for a visit of DAL to the European Center for Geodynamics and Seismology, April-May 2004. This work was also supported in the UK by NERC grant NER/A/S/2001/01166 to PJC, and in the USA by NASA Solid Earth and Natural Hazards grant SENH-0225-0008 to GB.

References List

Altamimi, Z., P. Sillard, and C. Boucher, ITRF2000: A new release of the International Terrestrial Reference frame for earth science applications, *Journal of Geophysical Research-Solid Earth*, *107* (B10), no.-2214, doi: 10.1029/2001JB000561, 2002.

Argus, D.F., W.R. Peltier, and M.M. Watkins, Glacial isostatic adjustment observed using very long baseline interferometry and satellite laser ranging geodesy, *Journal of Geophysical Research-Solid Earth*, *104* (B12), 29077-29093, 1999.

Blewitt, G., GPS data processing methodology from theory to applications, in *GPS for Geodesy*, edited by A. Kleusberg, and P.J.G. Teunissen, Springer Verlag, New York, 1997.

Blewitt, G., Self-consistency in reference frames, geocenter definition, and surface loading of the solid Earth, *Journal of Geophysical Research-Solid Earth*, *108* (B2), 2103, doi: 10.1029/2002JB002082, 2003.

Blewitt, G., Y. Bock, and J. Kouba, Position Paper 2 Constructing the IGS Polyhedron by Distributed processing. Densification of the IERS Terrestrial reference frame through regional GPS networks, in *IGS Workshop*, 1994.

Blewitt, G., and P. Clarke, Inversion of Earth's changing shape to weigh sea level in static equilibrium with surface mass redistribution, *Journal of Geophysical Research-Solid Earth*, *108* (B6), 2311, doi:10.1029/2002JB002082, 2003.

Blewitt, G., M.B. Heflin, F.H. Webb, U.J. Lindqwister, and R.P. Malla, Global Coordinates with Centimeter Accuracy in the International Terrestrial Reference Frame Using Gps, *Geophysical Research Letters*, *19* (9), 853-856, 1992.

Blewitt, G., and D. Lavallée, Effect of annual signals on geodetic velocity, *Journal of Geophysical Research-Solid Earth*, *107* (B7), 2145, doi: 10.1029/2001JB000570, 2002.

Blewitt, G., D. Lavallée, P. Clarke, and K. Nurutdinov, A new global mode of Earth deformation: Seasonal cycle detected, *Science*, *294* (5550), 2342-2345, 2001.

Boucher, C., and P. Sillard, Synthesis of submitted geocenter time series, in *International Earth Rotation Service Technical Note 25*, edited by J. Ray, pp. 15-21, International Earth Rotation Service, Paris, 1999.

Bouillé, F., A. Cazenave, J.M. Lemoine, and J.F. Cretaux, Geocentre motion from the DORIS space system and laser data to the Lageos satellites: comparison with surface loading data, *Geophysical Journal International*, *143* (1), 71-82, 2000.

Chen, J.L., C.R. Wilson, R.J. Eanes, and R.S. Nerem, Geophysical interpretation of observed geocenter variations, *Journal of Geophysical Research-Solid Earth*, *104* (B2), 2683-2690, 1999.

Cheng, M.K., Geocenter Variations from Analysis of TOPEX/POEIDON SLR Data, *IERS Technical Note, 25* (IERS Analysis Campaign to Investigate Motions of the Geocenter), 39-44, 1999.

Clarke, P.J., D. Lavallée, G. Blewitt, T. van Dam, and J. Wahr, Effect of gravitational consistency and mass conservation on seasonal surface mass loading models, *Geophysical Research Letters, in press*, 2005.

Cretaux, J.F., L. Soudarin, F.J.M. Davidson, M.C. Gennero, M. Berge-Nguyen, and A. Cazenave, Seasonal and interannual geocenter motion from SLR and DORIS measurements: Comparison with surface loading data, *Journal of Geophysical Research-Solid Earth, 107* (B12), 2374, doi:10.1029/2002JB001820, 2002.

Davies, P., and G. Blewitt, Methodology for global geodetic time series estimation: A new tool for geodynamics, *Journal of Geophysical Research-Solid Earth, 105* (B5), 11083-11100, 2000.

Davis, J.L., P. Elosequi, J.X. Mitrovica, and M.E. Tamisiea, Climate-driven deformation of the solid Earth from GRACE and GPS, *Geophysical Research Letters, 31* (24), art. no.-L24605, 2004.

Diziewonski, A., and D.L. Anderson, Preliminary Reference Earth model, *Phys. Earth Planets Inter., 25*, 297-356, 1981.

Dong, D., J.O. Dickey, Y. Chao, and M.K. Cheng, Geocenter variations caused by atmosphere, ocean and surface ground water, *Geophysical Research Letters, 24* (15), 1867-1870, 1997.

Dong, D., P. Fang, Y. Bock, M.K. Cheng, and S. Miyazaki, Anatomy of apparent seasonal variations from GPS-derived site position time series, *Journal of Geophysical Research-Solid Earth, 107* (B4), 2075, doi: 10.1029/2001JB000573, 2002.

Dong, D., T. Yunck, and M. Heflin, Origin of the international Terrestrial Reference Frame, *Journal of Geophysical Research-Solid Earth, 108* (B4), 2200, doi:10.1029/2002JB002035, 2003.

Farrell, W.E., Deformation of the earth by surface loads, *Reviews of Geophysics, 10*, 761-797, 1972.

Heflin, M., D.F. Argus, D.C. Jefferson, F.H. Webb, and J.F. Zumberge, Comparison of a GPS-defined global reference frame with ITRF2000, *GPS Solutions, 6* (72-75), 2002.

Heflin, M., W.I. Bertiger, G. Blewitt, A.P. Freedman, K.J. Hurst, S.M. Lichten, U.J. LIndqwister, Y. Vigue, F.H. Webb, T. Yunck, and J.F. Zumberge, Global Geodesy Using GPS without Fiducial Sites, *Geophysical Research Letters, 19,* 131-134, 1992.

Heflin, M., and M. Watkins, Geocenter Estimates from the Global Positioning System, *IERS Technical Note, 25* (IERS Analysis Campaign to Investigate Motions of the Geocenter), 55-70, 1999.

Kalnay, E., M. Kanamitsu, R. Kistler, W. Collins, D. Deaven, L. Gandin, M. Iredell, S. Saha, G. White, J. Woollen, Y. Zhu, M. Chelliah, W. Ebisuzaki, W. Higgins, J. Janowiak, K.C. Mo, C. Ropelewski, J. Wang, A. Leetmaa, R. Reynolds, R. Jenne, and D. Joseph, The NCEP/NCAR 40-year reanalysis project, *Bulletin of the American Meteorological Society*, *77* (3), 437-471, 1996.

Kedar, S., G.A. Hajj, B.D. Wilson, and M.B. Heflin, The effect of the second order GPS ionospheric correction on receiver positions, *Geophysical Research Letters*, *30* (16), art. no.-1829, 2003.

Lambeck, K., *Geophysical Geodesy; The Slow Deformations of the Earth*, Oxford Univ. Press, New York, 1980.

Lavallée, D., *Tectonic Plate Motions from Global GPS Measurements*, Ph. D. Thesis, University of Newcastle upon Tyne, 2000.

Lavallée, D., and G. Blewitt, Degree-1 Earth deformation from very long baseline interferometry measurements, *Geophysical Research Letters*, *29* (20), 1967, doi:10.1029/2002GL015883, 2002.

Malla, R.P., S.C. Wu, and S.M. Lichten, Geocenter location and variations in the Earth orientation using global positioning system measurements, *Journal of Geophysical Research-Solid Earth, 98* (B3), 4611-4618, 1993.

McCarthy, D.D., and G. Petit, IERS Conventions (2003), International Earth Rotation and Reference Systems Service, Verlag des Bundesamt für Kartographie und Geodäsie, Frankfurt am Main, 2004.

Moore, P., and J. Wang, Geocentre variation from laser tracking of LAGEOS1/2 and loading data, *Integrated Space Geodetic Systems and Satellite Dynamics*, *31*, 1927-1933, 2003.

Pavlis, E.C., Fortnightly Resolution Geocenter Series: a Combined Analysis of Lageos 1 and 2 SLR Data (1993-1996), *IERS Technical Note, 25* (IERS Analysis Campaign to Investigate Motions of the Geocenter), 75-84, 1999.

Penna, N.T., and M.P. Stewart, Aliased tidal signatures in continuous GPS height time series, *Geophysical Research Letters, 30* (23), art. no.-2184, 2003.

Ray, J., IERS Analysis Campaign to Investigate Motions of the Geocenter, in *IERS Tech. Note. 25*, edited by J. Ray, International Earth Rotation Service, Obs. Paris., 1999.

Ray, J., D. Dong, and Z. Altamimi, IGS Reference Frames: Status and Future Improvements, *GPS Solutions, 8* (4), 10.1007/s10291-004-0110-x, 251-266, 2004.

Shmakin, A.B., P.C.D. Milly, and K.A. Dunne, Global Modeling of land water and energy balances. Part III: Interannual variability, *Journal of Hydrometeorology, 3* (3), 311-321, 2002.

Stammer, D., R. Davis, L.-L. Fu, R. Fukumori, T. Giering, J. Lee, J. Marotzke, J. Marshall, D. Menemenlis, P. Niiler, C. Wunsch, and V. Zlotnicki, The Consortium for Estimating the Circulation and Climate of the Ocean (ECCO), Report 1, in *The ECCO Report Series*, 1999.

Tapley, B.D., S. Bettadpur, M. Watkins, and C. Reigber, The gravity recovery and climate experiment: Mission overview and early results, *Geophysical Research Letters*, *31* (9), art. no.-L09607, 2004.

Tregoning, P., and T. van Dam, The effects of atmospheric pressure loading and 7-parameter transformations on estimates of geocenter motion and station heights from space-geodetic observations, *Journal of Geophysical Research, In Press*, 2005.

Trupin, A.S., M.F. Meir, and J. Wahr, Effects of melting glaciers on the Earth's rotation and gravitational field: 1965-1984, *Geophysical Journal International*, *108*, 1-15, 1992.

Vigue, Y., S.M. Lichten, G. Blewitt, M.B. Heflin, and R.P. Malla, Precise Determination of Earths Center of Mass Using Measurements from the Global Positioning System, *Geophysical Research Letters*, *19* (14), 1487-1490, 1992.

Watkins, M.M., and R.J. Eanes, Long term changes in the Earth's shape, rotation, and geocenter, *Advances in Space Research*, *13* (11), 251-255, 1993.

Watkins, M.M., and R.J. Eanes, Diurnal and Semidiurnal Variations in Earth Orientation Determined from Lageos Laser Ranging, *Journal of Geophysical Research-Solid Earth*, *99* (B9), 18073-18079, 1994.

Watkins, M.M., and R.J. Eanes, Observations of tidally coherent diurnal and semidiurnal variations in the geocenter, *Geophysical Research Letters*, *24* (17), 2231-2234, 1997.

Wdowinski, S., Y. Bock, J. Zhang, P. Fang, and J. Genrich, Southern California Permanent GPS Geodetic Array: Spatial filtering of daily positions for estimating coseismic and postseismic displacements induced by the 1992 Landers earthquake, *Journal of Geophysical Research-Solid Earth*, *102* (B8), 18057-18070, 1997.

Wu, X.P., D.F. Argus, M.B. Heflin, E.R. Ivins, and F.H. Webb, Site distribution and aliasing effects in the inversion for load coefficients and geocenter motion from

GPS data, *Geophysical Research Letters*, *29* (24), 2210, doi:10.1029/2002GL016324, 2002.

Wu, X.P., M.B. Heflin, E.R. Ivins, D.F. Argus, and F.H. Webb, Large-scale global surface mass variations inferred from GPS measurements of load-induced deformation, *Geophysical Research Letters*, *30* (14), 1742, doi:10.1029/2003GL017546, 2003.

Zumberge, J.F., M.B. Heflin, D.C. Jefferson, M.M. Watkins, and F.H. Webb, Precise point positioning for the efficient and robust analysis of GPS data from large networks, *Journal of Geophysical Research-Solid Earth*, *102* (B3), 5005-5017, 1997.

Figure 1. Graphical representation of the displacements within a geodetic network due to the changing location of the center of mass of the surface load. CM is the center of mass of the solid Earth + load, the origin of satellite orbits which is essentially a kinematic fixed point in space. Two quite different expressions are observed, the displacement of the center of the solid Earth (CE) and the deformation of the solid Earth

Figure 2. Number of sites in each analysis center weekly solution for the period 1997.25-2004.25. Values are given after outlier rejection and elimination of sites with less than 104 weekly observations or less than 2.5 years of data.

Figure 3. Percentage of all analysis center sites in the hemisphere centered on the positive x, y and z axes respectively for the period 1997.25-2004.25. The 50% line represents the ideal situation of a well distributed network.

Figure 4. JPL geocenter formal error for the period 1997.25-2004.25: top “network shift” method, middle “degree-1 deformation” method, and bottom “CM method”. x formal error is plotted with a dotted line, y with a dashed line and z with a solid line.

Figure 5. SIO geocenter formal error for the period 1997.25-2004.25: top “network shift” method, middle “degree-1 deformation” method, and bottom “CM method”. x formal error is plotted with a dotted line, y with a dashed line and z with a solid line.

Figure 6. Top; normalized square root annual load degree amplitudes in units of mm of seawater. Square points: ocean load, diamonds: atmosphere, triangles: continental water and open circles: total load. Filled circles are the equilibrated total load. Bottom: power spectra of equilibrated total load model predicted $\Delta\mathbf{r}_{CF-CM}$ variations.

Figure 7. Histogram of $\Delta\mathbf{r}_{CF-CM}$ annual amplitude differences (mm) between those estimated from the synthetic data and the true value used to create the data. Shaded bars indicate that in addition to degree-1 deformation, degree-2 deformations were also estimated. Error bars are 1 standard deviation.

Figure 8. Histogram of $\Delta\mathbf{r}_{CF-CM}$ annual phase differences (°) between those estimated from the synthetic data and the true value used to create the data. Dotted outline bars indicate that in addition to degree-1 deformation, degree-2 deformations were also estimated. Error bars are 1 standard deviation.

Figure 9. Average power spectra of estimated scale, a) for the synthetic GPS data and b) for the real GPS data. Scale estimated with the network shift approach is plotted with a solid line + points, degree-1 deformation with a dotted line + points and CM method with a dashed line + points. The two lowermost solid lines (without points) in both plots are the degree-1 and CM deformation approaches where degree-2 is also estimated. The horizontal dot-dashed line in a) is the 5% significance level assuming background white noise with a variance estimated from the background spectra.

Figure 10. Histogram of GPS estimated $\Delta\mathbf{r}_{CF-CM}$ annual amplitude (mm). Shaded bars indicate that in addition to degree-1 deformation, degree-2 deformations were also estimated. Error bars are 1 standard deviation. Solid horizontal lines are the mean SLR estimates discussed in the text. Dotted horizontal lines are the equilibrated load model predicted values of $\Delta\mathbf{r}_{CF-CM}$ annual amplitude.

Figure 11. Histogram of estimated $\Delta\mathbf{r}_{CF-CM}$ annual phase (º). Dotted outline bars indicate that in addition to degree-1 deformation, degree-2 deformations were also estimated. Error bars are 1 standard deviation. Solid horizontal lines are the mean SLR estimates discussed in the text. Dotted horizontal lines are the equilibrated load model predicted values of $\Delta\mathbf{r}_{CF-CM}$ annual phase**.**

Table 1. Mean geocenter formal error for the period 1997.25-2004.25.

Analysis	Network Shift			Degree-1 Deformation			CM Method		
Center	X	Y	Z	X	Y	Z	X	Y	Z
emr	10.73	11.62	28.56	10.62	11.45	10.87	9.33	6.64	6.49
esa	7.56	7.53	33.67	10.58	10.74	10.19	9.81	5.49	5.14
gfz	6.26	6.18	6.85	6.47	7.56	7.24	3.22	3.78	3.56
jpl	6.12	5.96	6.20	6.97	6.67	6.31	3.51	3.23	3.09
ngs	11.65	11.29	33.41	9.82	9.60	9.15	9.35	6.78	6.25
sio	5.68	5.52	16.90	4.85	4.77	4.68	4.78	3.10	2.95

Table 2. Annual amplitude (mm) and phase (º) of load model used to create synthetic geodetic loading data. Amplitude and phase are defined by $A\cos[2\pi((t-t_0)-\Phi]$ where t_0 is 1 January.

Model	$\Delta\mathbf{r}_{CF-CM}$ Annual Amplitude			$\Delta\mathbf{r}_{CF-CM}$ Annual phase º		
	X	Y	Z	X	Y	Z
Atmosphere	0.35	1.37	1.02	159	170	154
Continental Water	0.80	0.73	2.39	234	103	255
Ocean Bottom Pressure	0.92	0.38	0.10	197	201	78
Total load	1.86	2.00	2.33	205	157	229
Equilibrated total load	2.35	2.25	2.72	207	160	231

Table 3. Mean and weighted RMS (WRMS) estimated analysis center $\Delta\mathbf{r}_{CF-CM}$ annual amplitude (mm) and phase (º) for the period 1997.25-2004.25. Amplitude and phase are defined by $A\cos[2\pi((t-t_0)-\Phi]$ where t_0 is 1 January.

All Analysis Centers						
	Δr_{CF-CM} Annual Amplitude			Δr_{CF-CM} Annual Phase		
	Mean	**σ**	**WRMS**	**Mean**	**σ**	**WRMS**
Network shift						
x	4.28	0.2	1.8	205	3	15
y	7.45	0.2	1.1	158	2	17
z	8.35	0.3	2.0	235	2	108
Degree-1 deformation method + degree 2 of total load						
x	3.71	0.2	1.2	221	3	23
y	2.52	0.2	1.3	183	5	39
z	10.59	0.2	5.7	215	1	10
CM method + degree 2 of total load						
x	1.93	0.1	0.9	218	3	19
y	3.30	0.1	0.5	166	2	21
z	5.05	0.1	3.8	234	1	24

All Analysis Centers except ESA						
	Δr_{CF-CM} Annual Amplitude			Δr_{CF-CM} Annual Phase		
	Mean	**σ**	**WRMS**	**Mean**	**σ**	**WRMS**
Network Shift						
x	4.68	0.2	1.9	208	3	11
y	7.57	0.2	1.3	155	2	17
z	8.01	0.3	1.0	270	2	65
Degree-1 deformation method + degree 2 of total load						
x	3.82	0.2	1.2	220	3	24
y	2.76	0.2	1.2	184	5	39
z	9.20	0.2	3.6	214	1	13
CM method + degree 2 of total load						
x	2.23	0.1	0.4	218	3	20
y	3.21	0.1	0.5	161	2	19
z	4.33	0.1	1.8	251	2	21

Analysis Centers ESA and SIO Excluded						
	Δr_{CF-CM} Annual Amplitude			Δr_{CF-CM} Annual Phase		
	Mean	**σ**	**WRMS**	**Mean**	**σ**	**WRMS**
Network Shift						
x	3.93	0.3	1.7	206	4	16
y	6.98	0.3	1.0	156	2	21
z	7.80	0.3	0.5	287	2	41
Degree-1 deformation method + degree 2 of total load						
x	3.57	0.3	1.6	231	5	27
y	2.44	0.3	1.4	161	7	40
z	9.93	0.3	4.5	210	1	8
CM method + degree 2 of total load						
x	2.26	0.2	0.6	221	4	22

y	3.20	0.2	0.6	157	3	22
z	3.63	0.2	0.3	266	3	11

All Analysis Centers except ESA, degrees up to 6 estimated for SIO						
	Δr_{CF-CM} **Annual Amplitude**			Δr_{CF-CM} **Annual Phase**		
	Mean	**σ**	**WRMS**	**Mean**	**σ**	**WRMS**
Degree-1 deformation method + total load						
x	2.55	0.2	1.6	231	4	24
y	2.90	0.2	1.0	176	4	26
z	8.80	0.2	4.2	211	2	9
CM Method + total load						
x	2.10	0.2	0.6	222	4	21
y	3.23	0.1	0.5	163	2	22
z	3.86	0.2	0.8	257	2	22

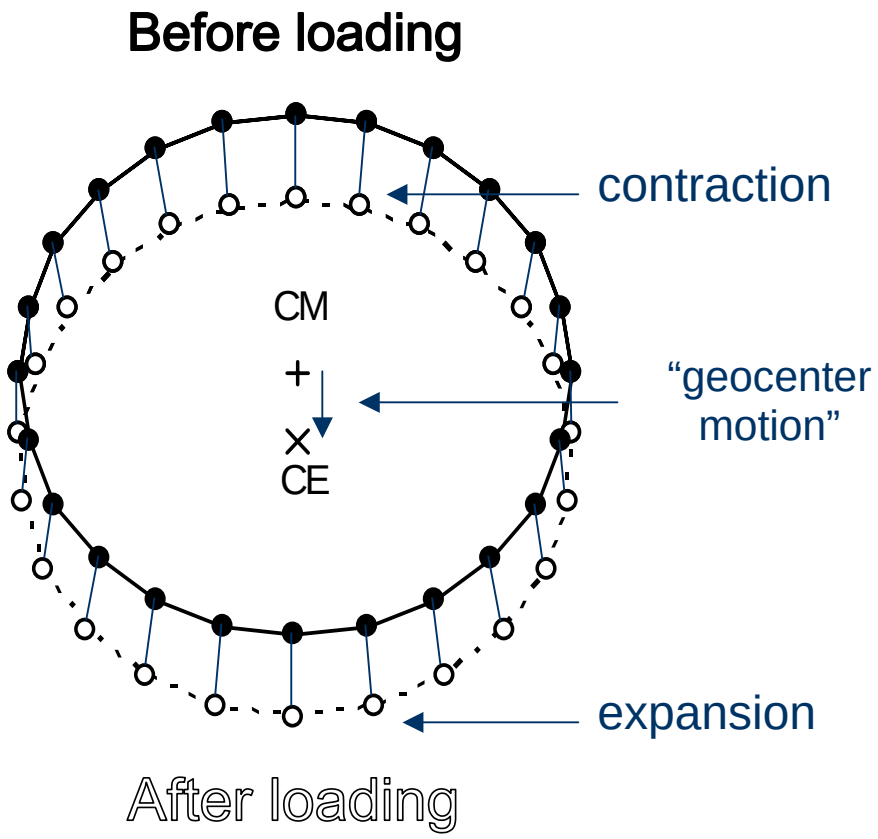

Figure 1. Graphical representation of the displacements within a geodetic network due to the changing location of the center of mass of the surface load. CM is the center of mass of the solid Earth + load, the origin of satellite orbits which is essentially a kinematic fixed point in space. Two quite different expressions are observed, the displacement of the center of the solid Earth (CE) and the deformation of the solid Earth.

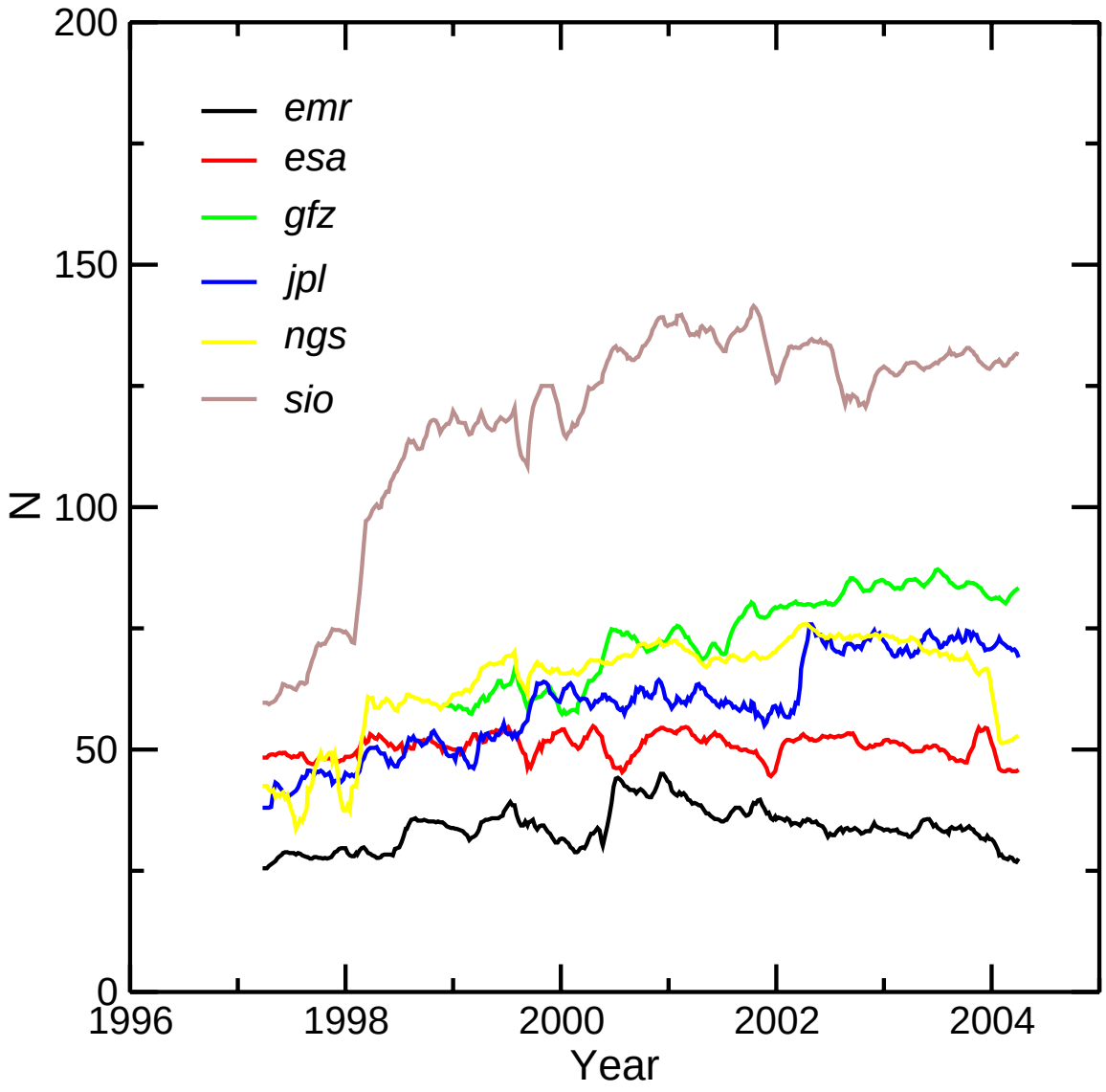

Figure 2. Number of sites in each analysis center weekly solution for the period 1997.25-2004.25. Values are given after outlier rejection and elimination of sites with less than 104 weekly observations or less than 2.5 years of data.

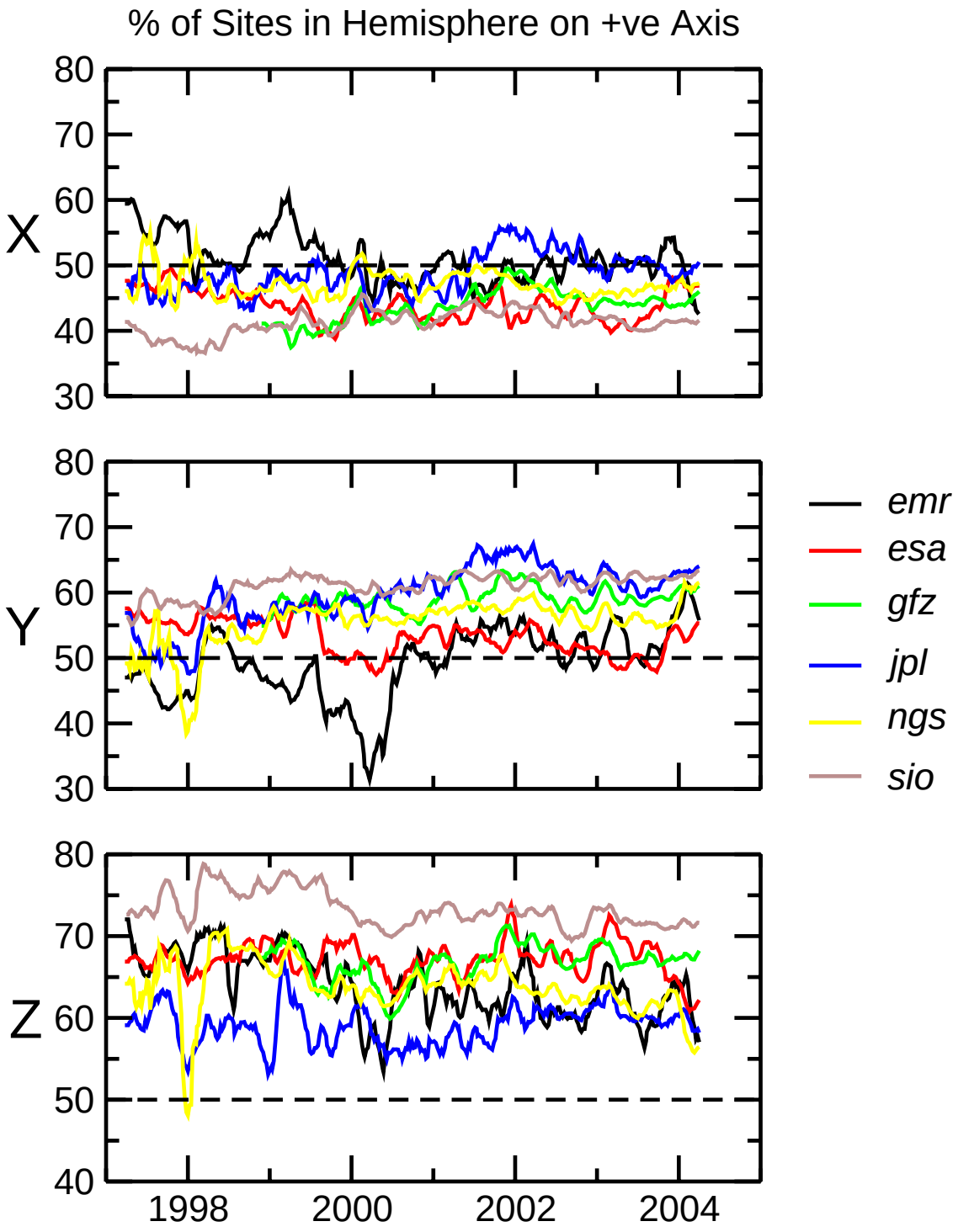

Figure 3. Percentage of all analysis center sites in the hemisphere centered on the positive x, y and z axes respectively for the period 1997.25-2004.25. The 50% line represents the ideal situation of a well distributed network.

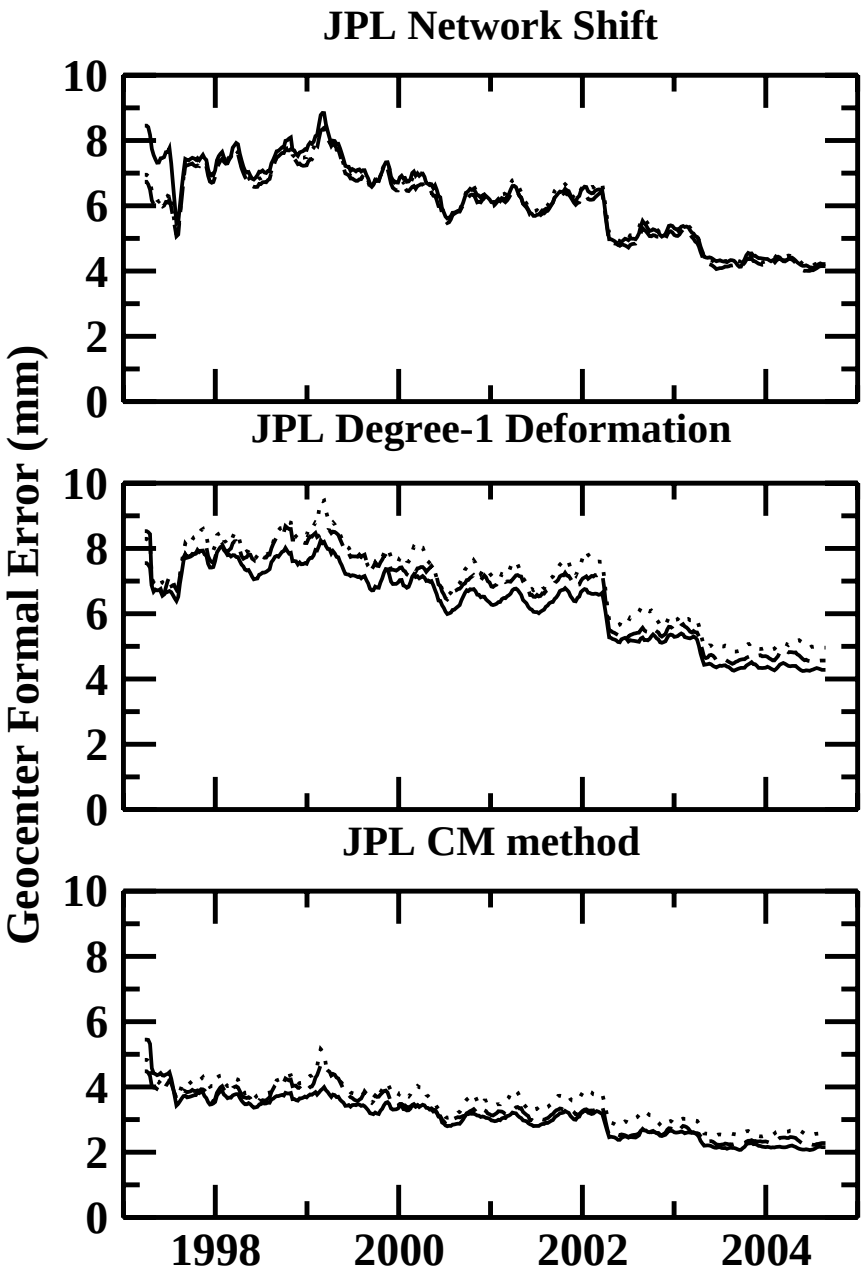

Figure 4. JPL geocenter formal error for the period 1997.25-2004.25: top "network shift" method, middle "degree-1 deformation" method, and bottom "CM method". x formal error is plotted with a dotted line, y with a dashed line and z with a solid line.

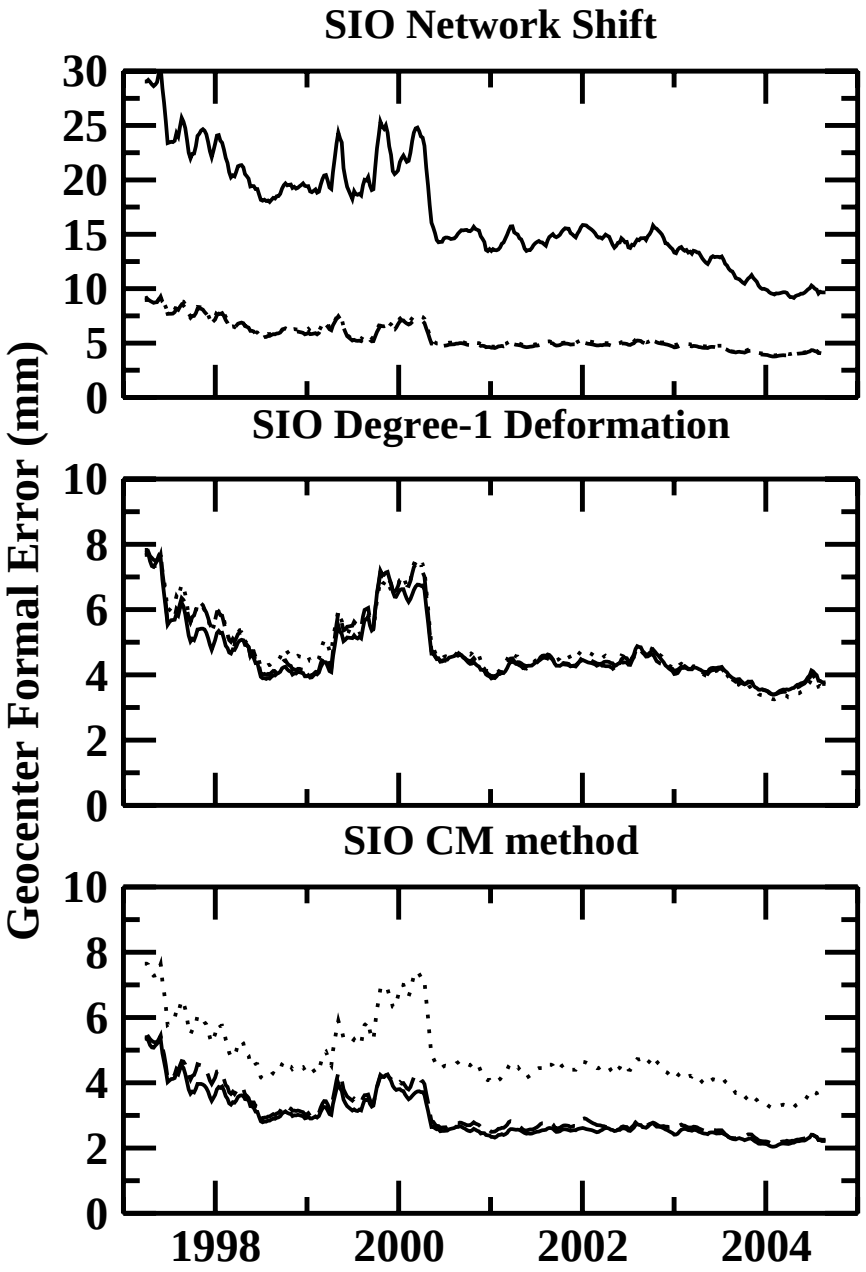

Figure 5. SIO geocenter formal error for the period 1997.25-2004.25: top "network shift" method, middle "degree-1 deformation" method, and bottom "CM method". x formal error is plotted with a dotted line, y with a dashed line and z with a solid line.

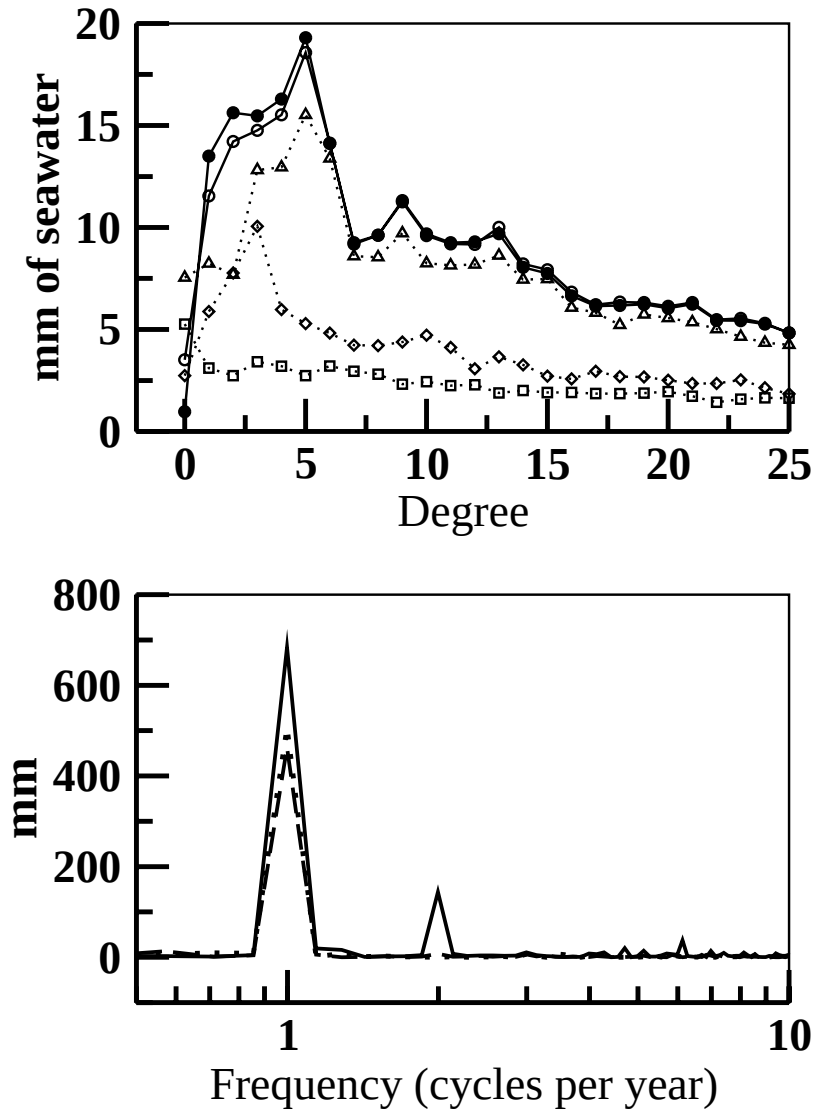

Figure 6. Top; normalized square root annual load degree amplitudes in units of mm of seawater. Square points: ocean load, diamonds: atmosphere, triangles: continental water and open circles: total load. Filled circles are the equilibrated total load. Bottom: power spectra of equilibrated total load model predicted $\Delta\mathbf{r}_{CF-CM}$ variations.

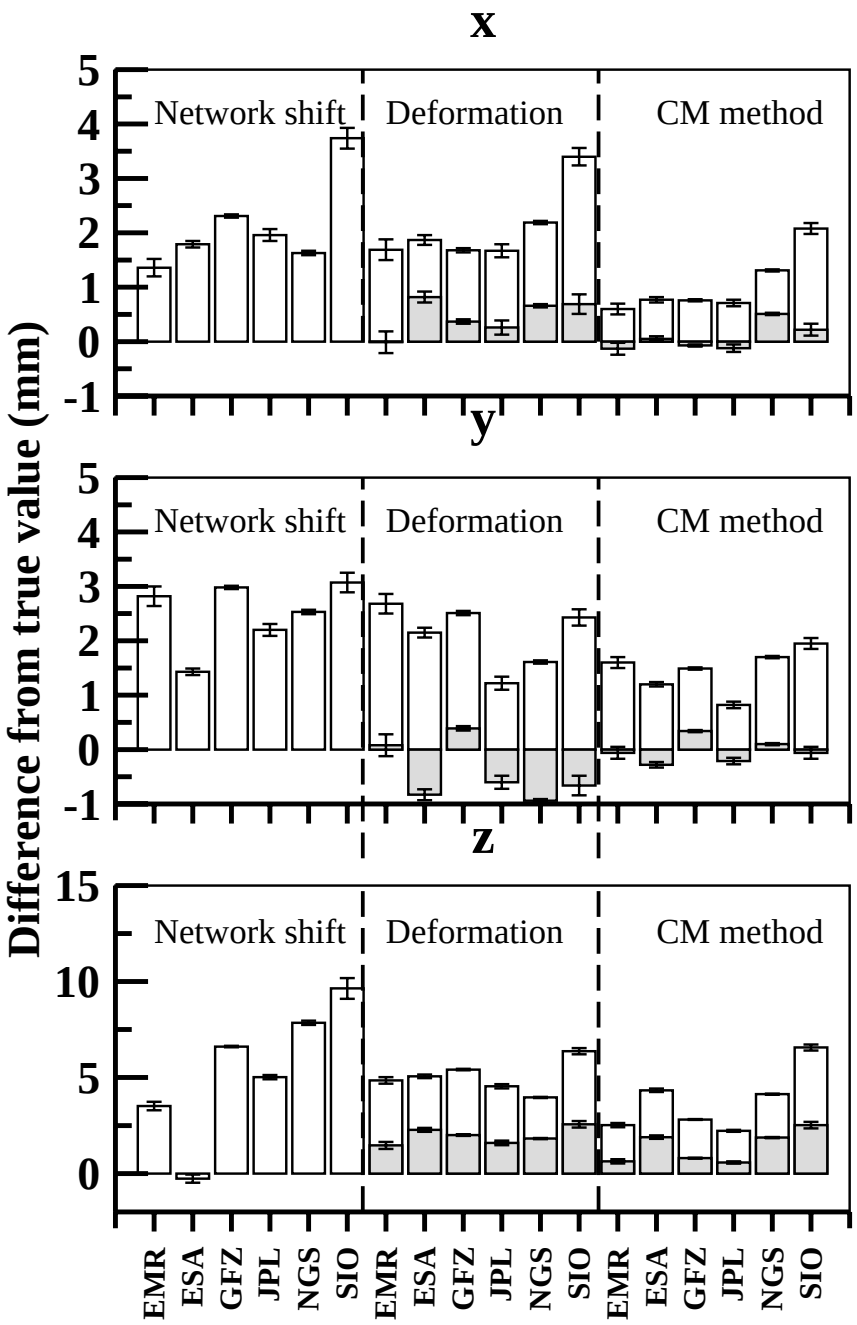

Figure 7. Histogram of $\Delta\mathbf{r}_{CF-CM}$ annual amplitude differences (mm) between those estimated from the synthetic data and the true value used to create the data. Shaded bars indicate that in addition to degree-1 deformation, degree-2 deformations were also estimated. Error bars are 1 standard deviation.

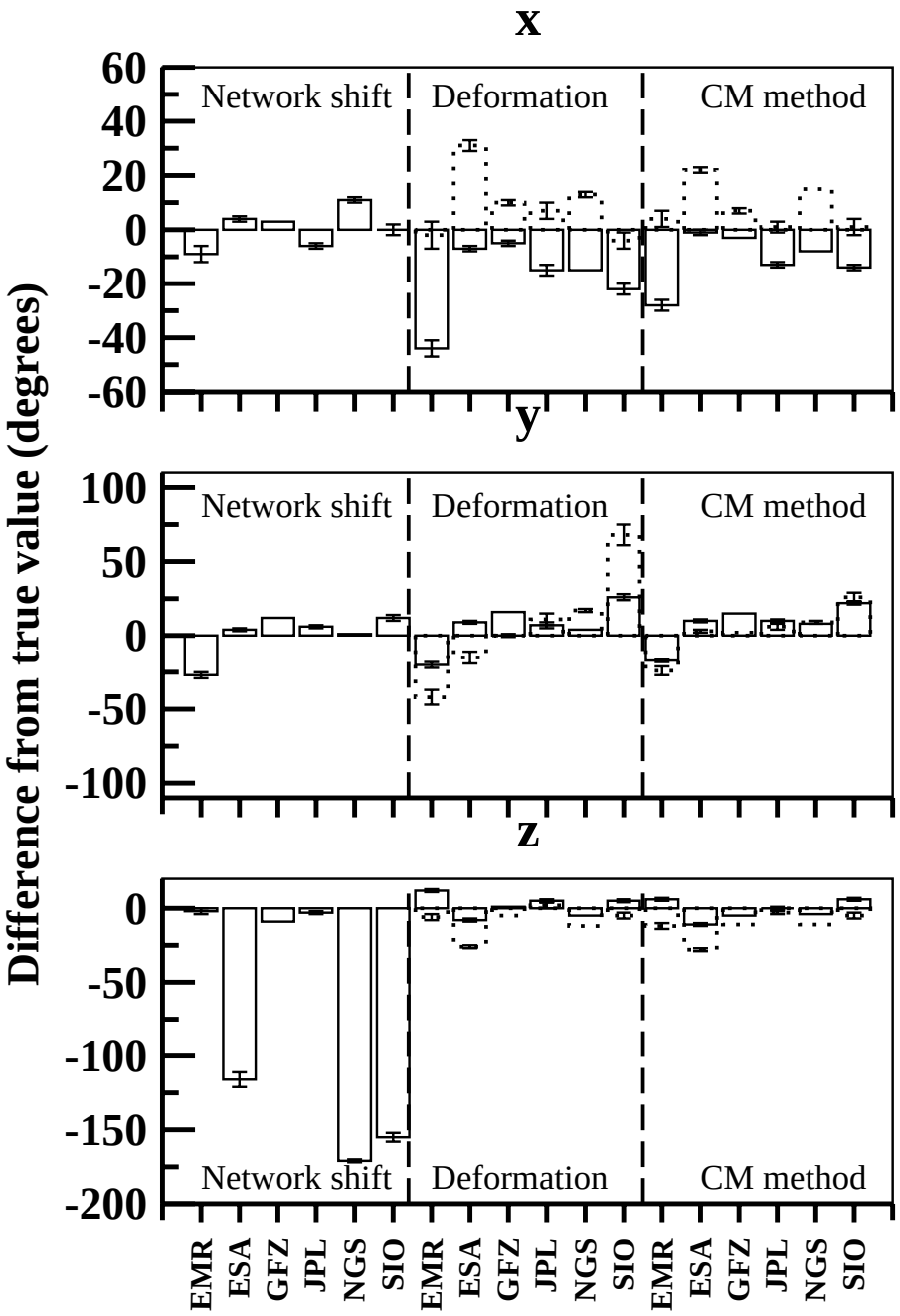

Figure 8. Histogram of $\Delta\mathbf{r}_{CF-CM}$ annual phase differences (º) between those estimated from the synthetic data and the true value used to create the data. Dotted outline bars indicate that in addition to degree-1 deformation, degree-2 deformations were also estimated. Error bars are 1 standard deviation.

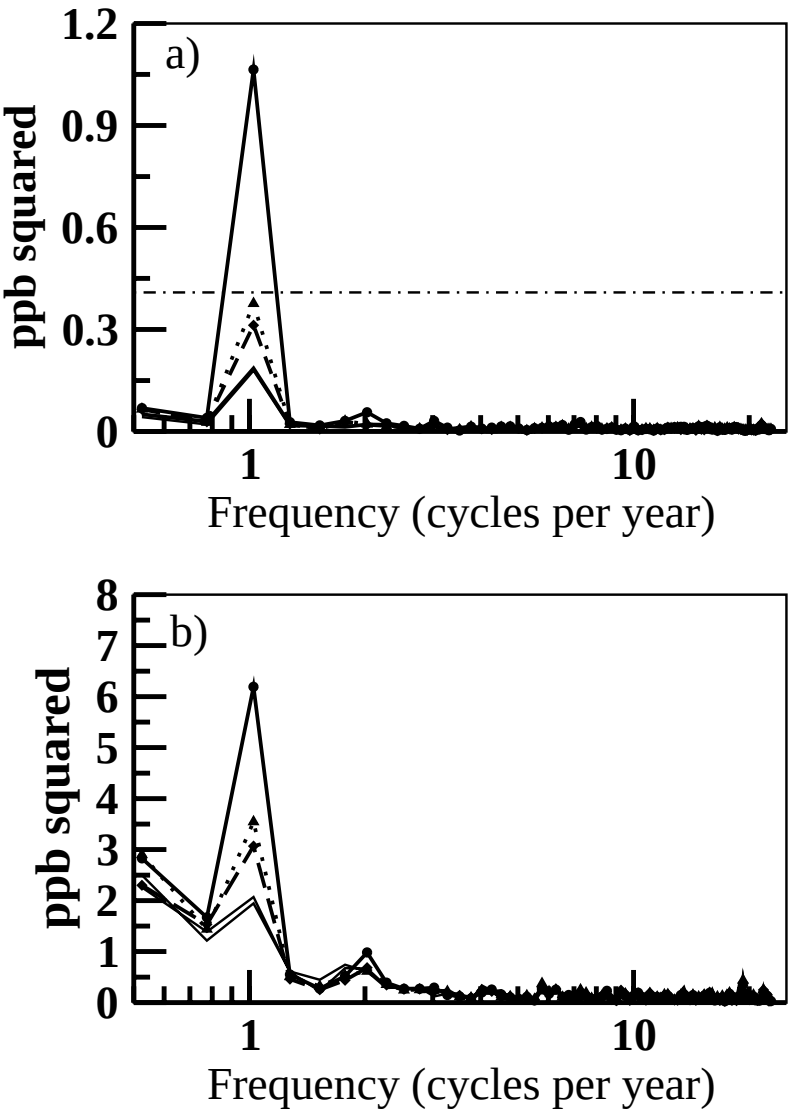

Figure 9. Average power spectra of estimated scale, a) for the synthetic GPS data and b) for the real GPS data. Scale estimated with the network shift approach is plotted with a solid line + points, degree-1 deformation with a dotted line + points and CM method with a dashed line + points. The two lowermost solid lines (without points) in both plots are the degree-1 and CM deformation approaches where degree-2 is also estimated. The horizontal dot-dashed line in a) is the 5% significance level assuming background white noise with a variance estimated from the background spectra.

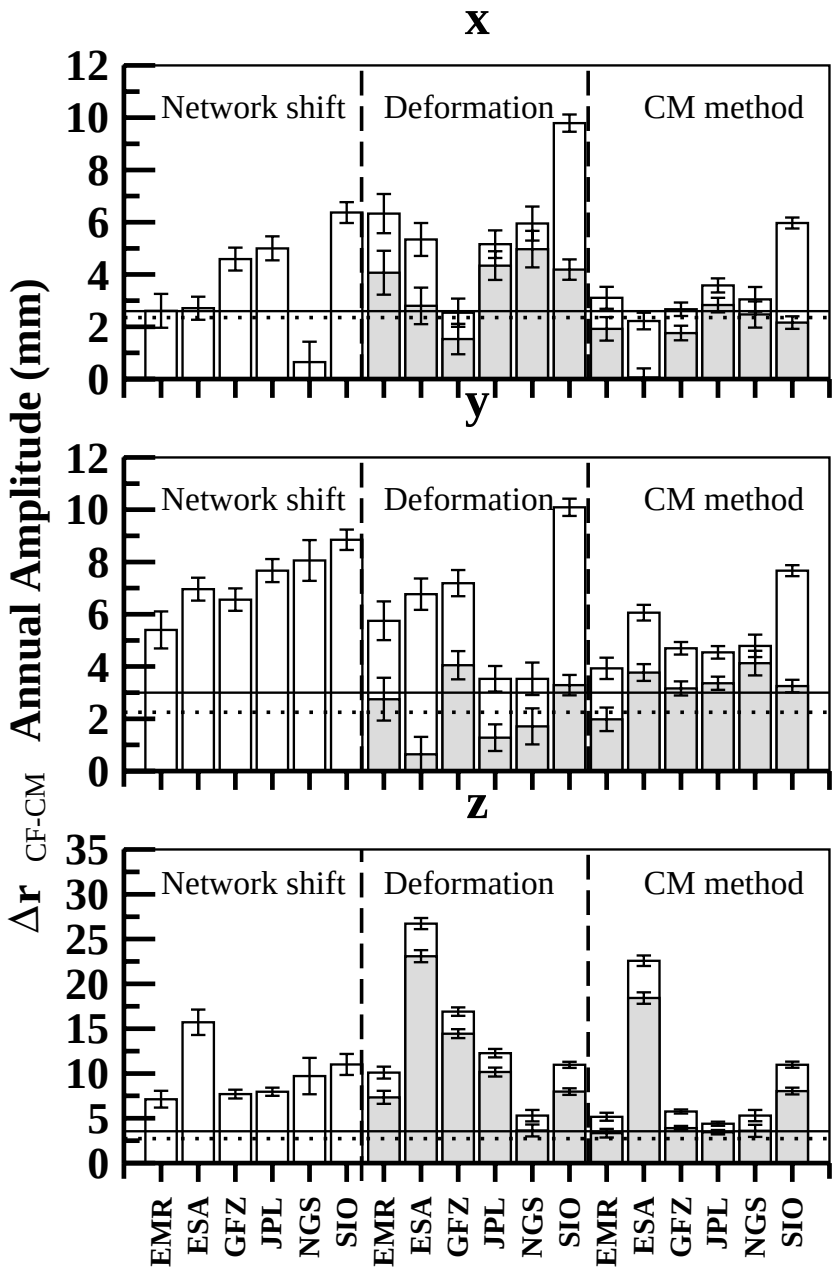

Figure 10. Histogram of GPS estimated $\Delta\mathbf{r}_{CF-CM}$ annual amplitude (mm). Shaded bars indicate that in addition to degree-1 deformation, degree-2 deformations were also estimated. Error bars are 1 standard deviation. Solid horizontal lines are the mean SLR estimates discussed in the text. Dotted horizontal lines are the equilibrated load model predicted values of $\Delta\mathbf{r}_{CF-CM}$ annual amplitude.

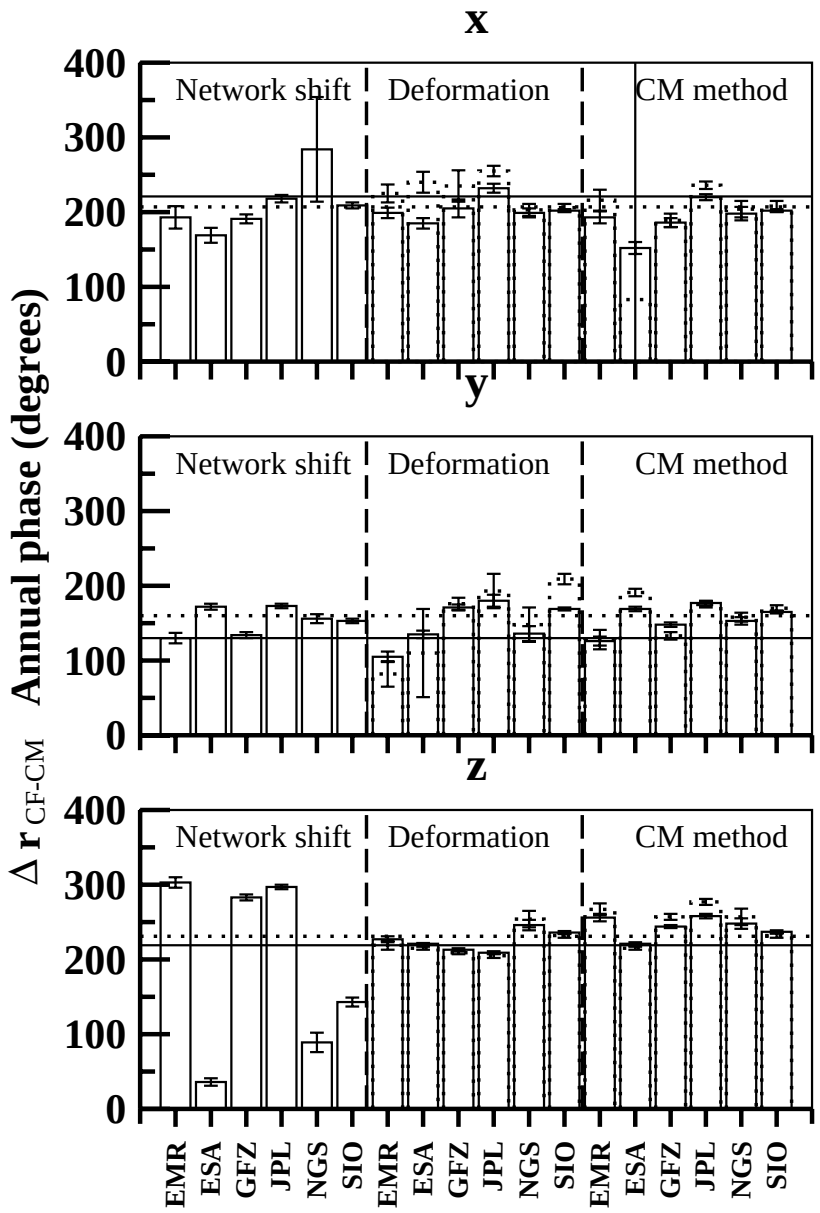

Figure 11. Histogram of estimated $\Delta\mathbf{r}_{CF-CM}$ annual phase (º). Dotted outline bars indicate that in addition to degree-1 deformation, degree-2 deformations were also estimated. Error bars are 1 standard deviation. Solid horizontal lines are the mean SLR estimates discussed in the text. Dotted horizontal lines are the equilibrated load model predicted values of $\Delta\mathbf{r}_{CF-CM}$ annual phase.